Lagrangian single-column modeling of Arctic airmass transformation during HALO-(*AC*)^3

Michail Karalis[1,], Gunilla Svensson[1,2], Manfred Wendisch[3], Michael Tjernström[1]

[1]Stockholm University, Department of Meteorology and Bolin Centre for Climate Research, Stockholm, Sweden

[2]KTH Royal Institute of Technology, Department of Engineering Mechanics, FLOW, Stockholm, Sweden

[3]Leipzig Institute for Meteorology (LIM), Leipzig University, Leipzig, Germany

July 23, 2025

We would like to thank the ACP editor and all anonymous referees for their insightful review of the manuscript. Below you may find our responses (regular font text) to each of the referee's remarks (gray text) along with the respective changes made in the manuscript (**"bold text"**)

Referee #1

Summary

In this study, Karalis and coauthors study the transformation of an air mass entering the Atlantic sector of the Arctic during March 2022. They use observations from the HALO-(AC)3 field campaign along with a single-column model to dissect the physical processes occurring within the air mass and validate the model simulations. They find that different physical processes influence the air mass cooling along its path, with near-surface radiative and turbulent cooling dominating over the ocean, and cloud processes and adiabatic cooling becoming more important as the air mass progresses into the marginal ice zone and sea ice areas. They also find that the single-column model generally simulates the air mass transformation realistically, but struggles to reproduce the stable boundary layer and is highly dependent on the vertical motion prescribed by the ERA5 reanalysis data used to force the model.

This study provides a unique perspective on Arctic air mass transformation, a process that is still not fully understood but is critically important to understanding the causes of Arctic-amplified warming. The paper is generally well-written and scientifically robust. I have a number of minor comments and technical corrections listed below. Once these comments are addressed, in my evaluation this will be a valuable addition to the literature on Arctic air mass transformation.

We thank the reviewer for their positive review and insightful comments which helped improve the state of the manuscript considerably.

Minor comments

- General comment: Is this air mass considered to be "fully transformed" at the end of the 12–14 March 2022 study period, or did it continue cooling after the HALO-(AC)3 sampling ended on 14 March? At the end of the study period, was the air temperature characteristic of a cold Arctic air mass, or was its thermal state more characteristic of an air mass still in transition from mid-latitude to Arctic conditions? If it continued cooling, do the authors expect that the dominant cooling processes at the end of the study period continued to be most important for air mass cooling as the air continued to reside in the Arctic? From Fig. 4 it appears the air mass was still cooling, albeit at possibly a cooler rate, at the end of the study period. I understand that further simulations outside the study period are likely outside of the scope of this study, but it would be useful to provide some discussion about these aspects for context.

A: Thank you for raising this point. The airmass is, indeed, not fully transformed by the end of the simulation period. With an integrated water vapor (IWV) content of 8 kg m^{-2}, it is still anomalously moist (and subsequently warm) compared to the 1979-2019 climatological median of approximately 2 kg m^{-2} (Rinke et al., 2021). The future of the remaining heat and moisture will be determined by:

1. Its residence time in the Arctic. Airmasses take, on average, 5 days to cross the Arctic (Woods and Caballero, 2016) . Depending on the dominant mechanisms in each case, this may not be enough time for an airmass to be entirely transformed by the time it exits the region. In this specific case, the second warm-air intrusion that took place the next day (March 15) will likely mix with the left-over moisture from the previous episode and cease the transformation process prematurely.
2. The large-scale dynamic conditions. The updraft that dominated the second half of the transformation forced a moisture loss of around 5 kg m^{-2}. If that were to be sustained for longer, IWV could drop to typical Arctic airmass values in the next 24 hours. In milder subsidence conditions, temperature changes would be driven mostly by radiative cooling (Fig AR1.1). The emitted longwave radiation, however, would grow weaker as the temperature drops and the liquid clouds dissipate, requiring more time for the transformation to reach completion.

We added the following lines in Sect. 3.3.6

L498-509: "It should be noted that, at the end of the the simulation period, the airmass has an IWV_{5km} of 8 kg m^{-2}, which makes it still anomalously moist (and subsequently warm) compared to the 1979-2019 climatological median of approximately 2 kg m^{-2} (Rinke et al., 2021). The airmass transformation is, therefore, not complete and could continue for several days as is typical for WAIs in the Atlantic sector (Woods and Caballero, 2016). In this specific case, the second warm-air intrusion that is set up to take place the next day (March 15) will likely mix with the left-over moisture from the previous episode and cease the transformation process prematurely. But large-scale dynamics are important for the future of the remaining heat and moisture even before the merge. The large-scale updraft that dominated the transformation over sea-ice resulted in a temperature decrease of 6 ºC, triple in magnitude that that exerted by radiation and turbulent mixing combined (Fig. C1). If the airmass continued to be lifted and, thus, losing heat and moisture at the same rate, IWV could drop to

typical Arctic airmass values in the next 24 hours. In milder subsidence conditions, temperature changes would be driven mostly by radiative cooling (Fig. C1). The emitted longwave radiation, however, would grow weaker as the temperature drops and the liquid clouds dissipate, requiring more time for the transformation to reach completion. ”

- General comment: The authors provide qualitative descriptions of which physical processes were most important for air mass cooling at different stages of its life cycle. Is it possible to integrate these contributions over time to provide a comparison of which processes contributed the most to cooling throughout the entire study period?

A: Thank you for this suggestion. We computed the contributions of the participating processes by integrating the temperature changes in time and height (up to 5 km). This shows adiabatic cooling as the biggest contributor to the airmass transformation, followed by radiation (Fig. AR1.1). The only consistent heat source for the airmass is latent heat release from cloud condensation which then drives the moisture depletion. We include the figure in Appendix C (Fig. C1)

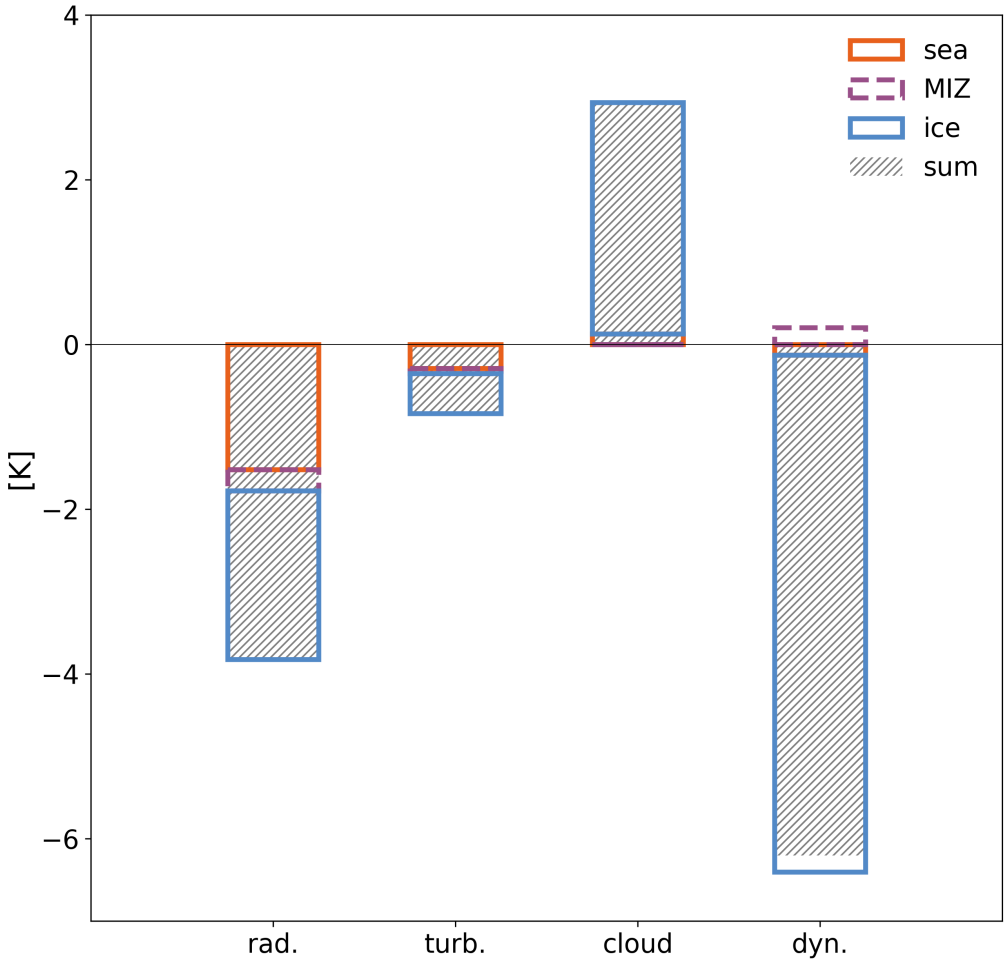

Figure AR1.1: Integrated temperature changes contributed by radiation, turbulence, cloud processes and adiabatic cooling. Different colors are used to show the changes per transformation leg (ocean, MIZ, ice) and hatches to show the sum over the entire transformation.

- L6: The meaning of "undistorted" air column isn't quite clear here and doesn't become apparent until later in the paper (e.g. L99–101, L112–118, L180–191). I suggest using the word "cohesive" in the abstract (as in L182) to be more clear.

A: Thank you. We changed it to the proposed phrasing (**L6**)

- L150–152: What type of adjustment is needed for the model to be able to produce realistic skin temperature values?

A: The surface energy budget from the incoming warm and moist airmass leads to a quick increase in the skin temperature. Skin temperature is the variable through which the air-column is coupled to the surface as it participates in the calculation of surface energy fluxes. Thus, the fast adjustment of the surface to the overlying column becomes problematic when trying to study the Lagrangian airmass transformation, big part of which is the response of the airmass to the constantly varying surface conditions.

We kept the skin temperature from increasing by initializing the sea-ice with larger internal energy values or, in simpler terms, colder sea-ice temperatures than the reanalysis in the representative region. This causes the downward conductive heat flux to counterbalance the incoming energy and maintains a colder skin temperature. For reference, for the 25 h long “ice” leg, the simulated mean sea-ice temperature goes from approximately -32 ºC to -28 ºC, the sea-ice surface temperature increases from -33 ºC to -13 ºC while the snow skin temperature adjusts at approximately -8 ºC and remains constant for the entire leg (Fig. AR1.2). This procedure gives a more advanced coupling to the sea ice than the limited options through prescribing surface values. Fig. AR1.2 is now offered in Appendix B.

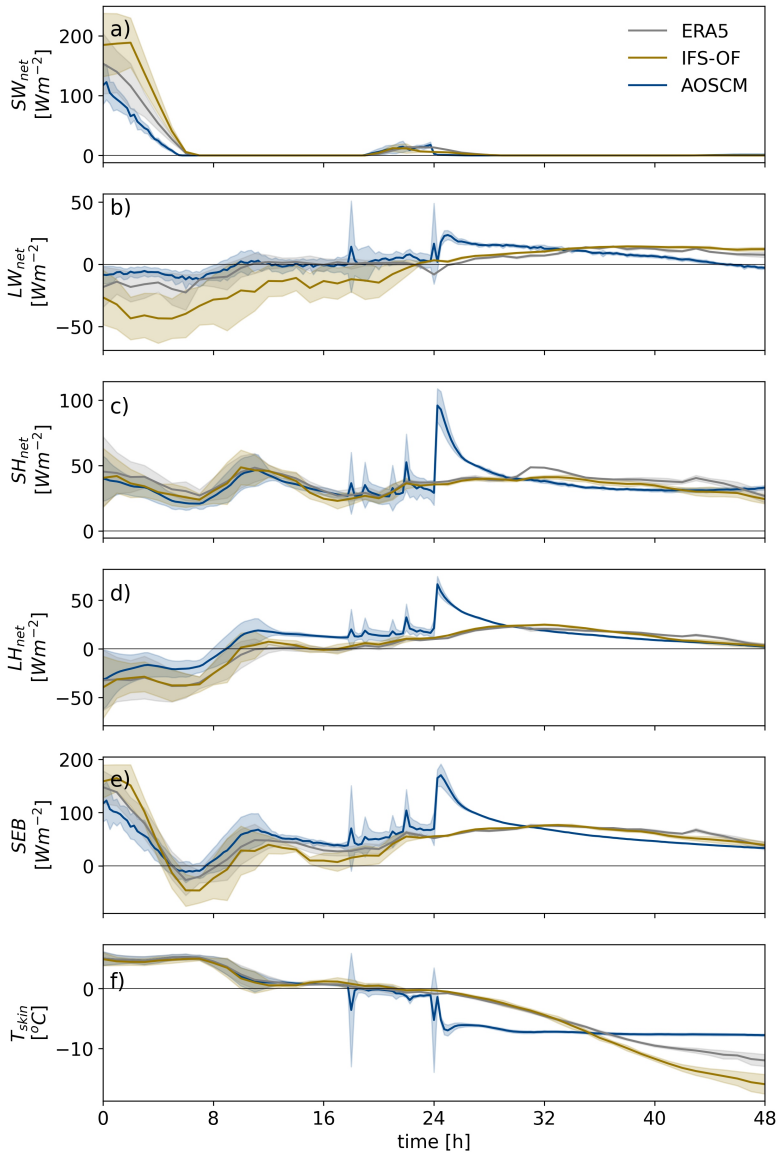

Figure AR1.2: Time-series of the surface a) shortwave radiative, b) longwave radiative, c) sensible heat, d) latent heat fluxes, e) the surface energy budget and f) the skin temperature along the trajectories. The AOSCM, ERA5 and IFS-OF are drawn with blue, grey and sand respectively.

This is not an optimal fix but, it helps realistically simulate the airmass Lagrangian evolution by ensuring fluxes of comparable magnitude to ERA5 and the operational forecast IFS-OF. Additionally, this treatment is specific to this application and this version of the AOSCM where LIM3 is used as a sea-ice model. In future studies, working with newer versions of AOSCM in which LIM3 has been replaced with SI3, we can achieve similar results by breaking up the airmass trajectory to smaller legs and re-initializing the sea-ice properties more frequently. We have added the following sentence in the manuscript.

L174-177: “ ~~ERA5 is also used for the initialization of sea-ice temperature, although an adjustment is necessary for the model to be able to produce realistic skin temperature values, comparable to the respective mean ERA5 values for each leg.~~ **We initialize the sea ice at lower temperatures than indicated by reanalysis. This causes the downward conductive heat flux to counterbalance the incoming energy, maintaining a colder skin temperature, comparable to the respective mean**

ERA5 values for each leg (Fig. B1f, Table 1). As a result, the surface fluxes are closer to ERA5 (Fig. B1a-e). ”

- L145–154: I'm not entirely clear on the mixture of data sources here. So ERA5 is used for SIC, then CMEMS is used to quantify snow on top of sea ice and sea ice thickness? So both the snow on sea ice and the sea ice thickness are taken into account by the AOSCM? This is also unclear in L364–366.

A: The AOSCM requires sea-ice and snow thickness information to be given as input. However, this information is not available in ERA5. Instead, we take characteristic values for the MIZ and sea-ice legs respectively from CMEMS. We used ERA5 to initialize sea-ice concentration but values are similar in both reanalyses.

We realize that merely describing the various datasets does not necessarily reflect the differences in the sea-ice properties between the different simulation legs. We, therefore, introduce Table 1. in Sect. 2.4 of the manuscript in which we explicitly present the values used for the sea-ice properties of each leg.

“

Table 1. Representative values for sea-ice and snow properties used in the coupled simulations.

	MIZ	ice
Sea-ice concentration	60 %	99 %
Ice thickness	0.90 m	2.1 m
Snow thickness	0.13 m	0.31 m
Skin temperature	~ -1.5 °C	~ -8 °C

”

- Fig. 2 and Fig. 3: Are these maps showing instantaneous snapshots of IVT, IWV, LWP, etc.? Or are these quantities integrated over time? Is the (Eulerian) ERA5 regular grid field of these values plotted, or are the values interpolated to the Lagrangian trajectories? I assume the cloud fields (LWP, IWP) and SEB values (SHF, LHF, etc.) are taken from ERA5, is this correct?

A: All variables shown in Fig. 2c and Fig. 3 are taken from ERA5. These plots show the Lagrangian evolution of each variable along and around the airmass trajectories rather than a snapshot of the fields at any specific moment. It may be helpful to think of the trajectories in these plots as a time axis. At each timestep the airmass around the trajectories is detected and visualized according to the airmass tracking method described in Sect. 2.3. These Lagrangian maps show the width of the airmass with respect to the width of the trajectory ensemble, with the latter representing the size of the air-column our study focuses on, and reveal the amount of variability that exists within the airmass. We have edited **Fig. 2c’s caption** to help the reader interpret the figure more easily.

“c) ~~temporal evolution and spatial variability of integrated water vapor transport (IVT). The trajectory ensemble is shown with black lines. Hatches mark the correlation range (see Sect. 2.3)~~

~~around the airmass at each timestep.~~ **Map of the temporal evolution and spatial variability of integrated water vapor transport (IVT). The trajectory ensemble, drawn with black lines, serves the purpose of a time axis. IVT changes in the direction parallel to the trajectories show the temporal evolution of the airmass. IVT changes in the direction perpendicular to the trajectories show the spatial variability of the airmass at the respective timestep (12/03/2022, 12 UTC at the southernmost point to 14/03/2022, 12 UTC at the northernmost). Hatches mark the correlation range showing areas around the trajectories of similar vertical structure at each timestep (see Sect. 2.3). "**

- L206–208: This is an interesting hypothesis about the quality controls in the assimilation scheme filtering the profiles out – is there any way to check this?

A: Ehrlich et al., (2025) reported that none of the dropsonde profiles collected during this WAI event were submitted to the Global Telecommunication System (GTS). Therefore, no observations from flights RF02, RF03 and RF04 were assimilated in ERA5 which makes their in-between mismatch a lot more reasonable. We update our statement about dropsonde assimilation and relevant discussion accordingly:

L233-235: "~~The profiles located on the eastern boundary of the airmass show a consistent mismatch with ERA5 data, in most cases, severely lacking in moisture content. It is likely that observations at these locations are capturing the steep moisture gradient at the airmass boundary, unable to be represented in ERA5 either due to i) ERA5's resolution or ii) the quality controls built in the assimilation scheme potentially filtering the profiles out triggered by large deviations between the observations and the forecasted values (Hersbach et al., 2020).~~**"**

"Observations from these research flights were not submitted to the Global Telecommunication System (GTS) for assimilation (Ehrlich et al., 2025) which explains why the observed steep moisture gradient at the airmass boundary is not represented in ERA5."

We also correct the following sentence in Sect. 2:

L105 - 106 : "The initialization of the trajectories at this location ~~serves a dual purpose: i) the use of more realistic ERA5 wind fields in this region at the time of initialization due to the abundance of dropsonde profiles available for assimilation (Hersbach et al., 2020), and ii)~~ **guarantees** more matches between trajectory and observational points which enables the comparison.**"**

We also remove the following sentence in Sect. 3.3.2:

L285-288(former): "T~~his abrupt change is coincident with the start of a new ERA5 assimilation window (at 9 UTC) and is, most probably, related to the adjustment of the airmass state to the numerous available dropsonde observations available over MIZ at that time.~~**"**

- L214–219: This paragraph is describing the cloud radiative effect – is it possible to directly calculate the cloud radiative effect and plot it on the maps?

A: We calculated cloud radiative forcing (CRF) for shortwave and longwave radiation CRF_{SW} = SW_{sfc}^{cld} - SW_{sfc}^{clr} and CRF_{LW} = LW_{sfc}^{cld} – LW_{sfc}^{clr} using ERA5 data (Fig. AR1.3). The intruding

airmass consistently contributes around 80 W m^{-2} uniformly across the transport corridor, wherever liquid clouds are present. We add this information in the discussion and offer the figure as supplementary material.

L244-252: "~~The spatial distribution of the cloud water within the airmass is also reflected in the net shortwave radiation flux at the surface (Fig. 3d) during daytime. On the western flank of the airmass, where the LWP is larger, less solar radiation reaches the surface but the down-welling long-wave radiation emitted by the liquid clouds changes the sign ofthe net surface long-wave flux to positive (Fig. 3e).~~ **The net shortwave radiation along the path of the airmass is presented in Fig. 3d. At the time of the event (March 12-14), the Arctic receives roughly 7 to 11.4 hours of daylight depending on the latitude of interest. Therefore, solar radiation is only relevant for small parts of the airmass transformation. The surface shortwave radiative flux is largest near the south end of the trajectories (200 W m−2). Its spatial distribution mimics that of the liquid cloud water within the airmass (Fig. 3b). On the western flank of the airmass, where the LWP is larger, the liquid cloud blocks approximately up to 300 W m−2 of solar radiation (Fig. A1). In contrast, the liquid cloud consistently casts a longwave radiative forcing of around 80 W m−2 (Fig. A1) which changes the sign of the net surface long-wave flux to positive (Fig. 3e).**

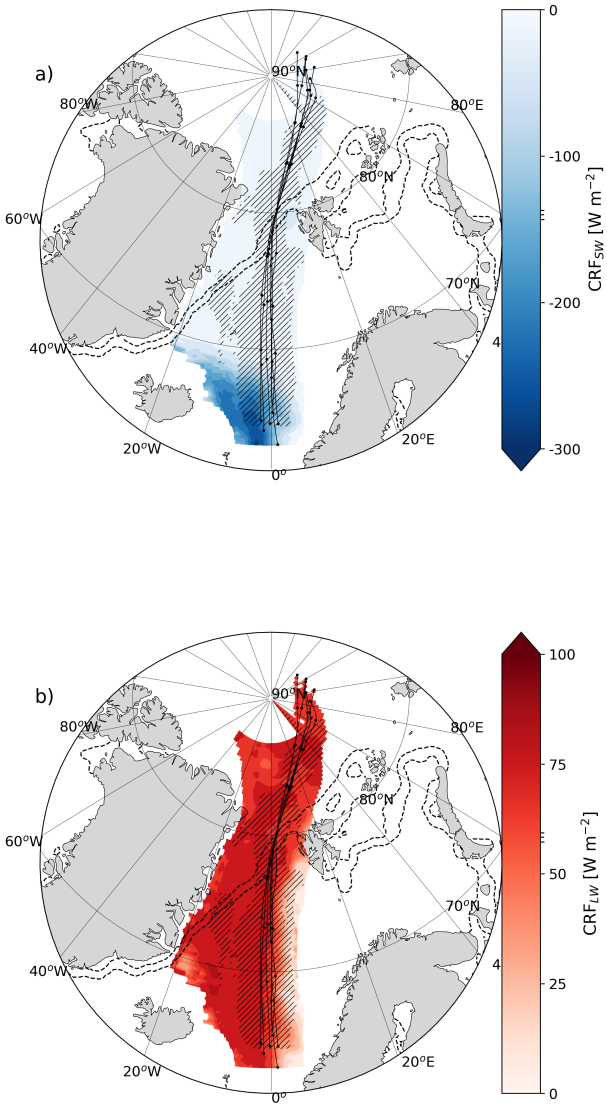

Figure AR1.3: Temporal evolution and spatial variability of the airmass during its poleward advection in terms of a) shortwave and b) long-wave radiative forcing. The trajectory ensemble is shown with black lines. Hatches mark the correlation range (see Sect. 2.3) around the airmass at each timestep. Square markers, when present, correspond to the observed values. Dashed contours show boundaries of the MIZ, corresponding to sea-ice concentration values 0.15 and 0.8 on March 13, at 12 UTC.

- Fig. 4: I don't quite understand how cloud liquid and ice are represented in Fig. 4. Does the shaded area represent the additional atmospheric water in ice or liquid phase, in addition to the vapor-phase water (IWV)?

A: That is correct, the thickness of the shaded area represents the integrated cloud water content (liquid and ice) and the texture represents the phase (dots for liquid, no dots for ice). This information is now clearly stated in the figure caption.

"The width of the shaded areas attached to the right of the thick solid lines represents the vertically integrated total water path (TWP). Dots are used to show the portion that is in liquid phase (LWP)."

- Fig. 4: It is difficult to distinguish between the faded perpendicular lines for AOSCM/ERA5/IFS. Perhaps some could be plotted as dotted or dashed lines to make them easier to tell apart? Does each of these lines represent a timestep, such that the wider spacing of the lines over sea ice can be interpreted as faster air mass cooling and drying? Is appears that the uncertainty range is greater for the AOSCM than the other two products, is that correct?

A: We replotted the faded perpendicular lines in different styles to make them more distinguishable from each other (AR1.4). Spaces between these lines represent time intervals of 1 hour. The reviewer is correct to note that when the spacing becomes wider, the transformation accelerates. We now note this in the caption of Fig. 4:

"The faded lines are plotted with a time-step of 1 h, therefore their density signifies the speed of the transformation. "

The AOSCM uncertainty range is indeed larger than ERA5 and IFS-OF and it encompasses the curves of ERA5 and IFS-OF, as well as observations. The magnitude of the AOSCM ensemble uncertainty varies with time as a result of variability in the initial conditions and forcing. This is discussed in the manuscript in lines **L293-299**. Among other changes in this section, following the referees' suggestions, we have also added:

L297-298: "The increase in the AOSCM ensemble uncertainty is the combined result of the variability in the ensemble's initial conditions and alongstream forcing.

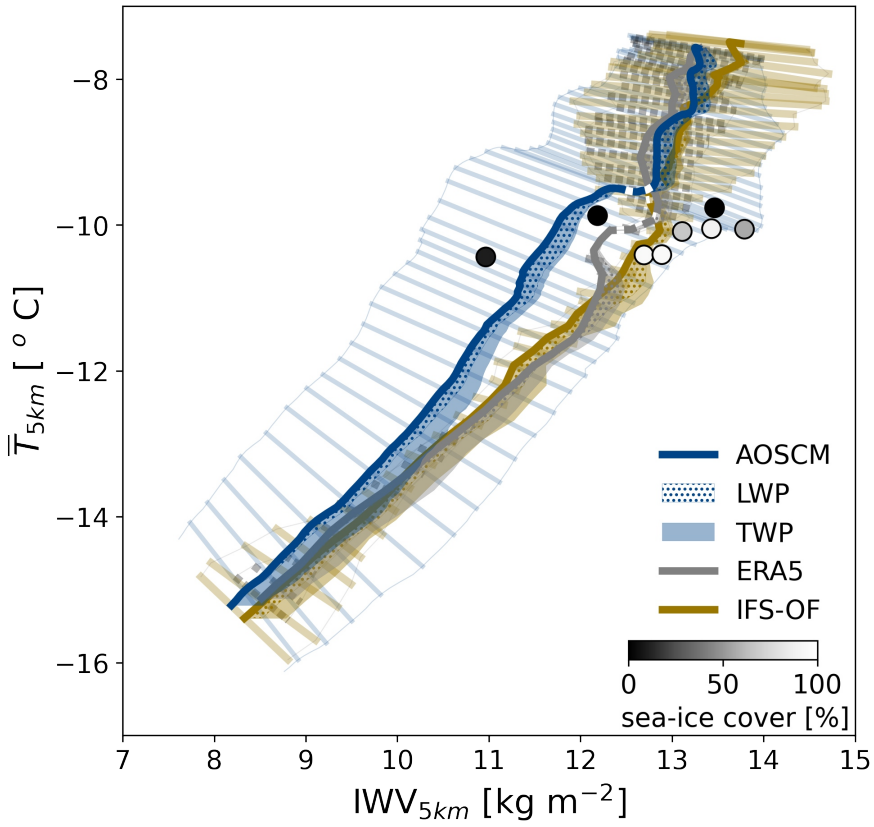

Figure AR1.4: Same as Fig. 4 in the manuscript with more distinguishable uncertainty range lines.

- L326–327: How was Bulk Richardson number = 0.25 chosen as the threshold for the boundary layer? Is this threshold based on previous studies?

A: This Bulk Richardson number threshold is used to diagnose the height of the boundary layer in ECMWF's Integrated Forecast System (IFS). IFS is the atmospheric component of AOSCM and the model used for the production of ERA5 and IFS-OF. Therefore, this diagnostic gives the most fair comparison of the boundary layer in all of the above products.

- Fig. 5: Is this figure created by averaging all the trajectories? Also, the uncertainty contours are difficult to see on the figure panels – perhaps they could be plotted with a darker color and/or thicker line.

A: Yes, the cross-sections presented in Fig. 5 are a product of averaging among the cross-sections of the individual trajectories. We made the uncertainty contours thicker so they can be more easily distinguished.

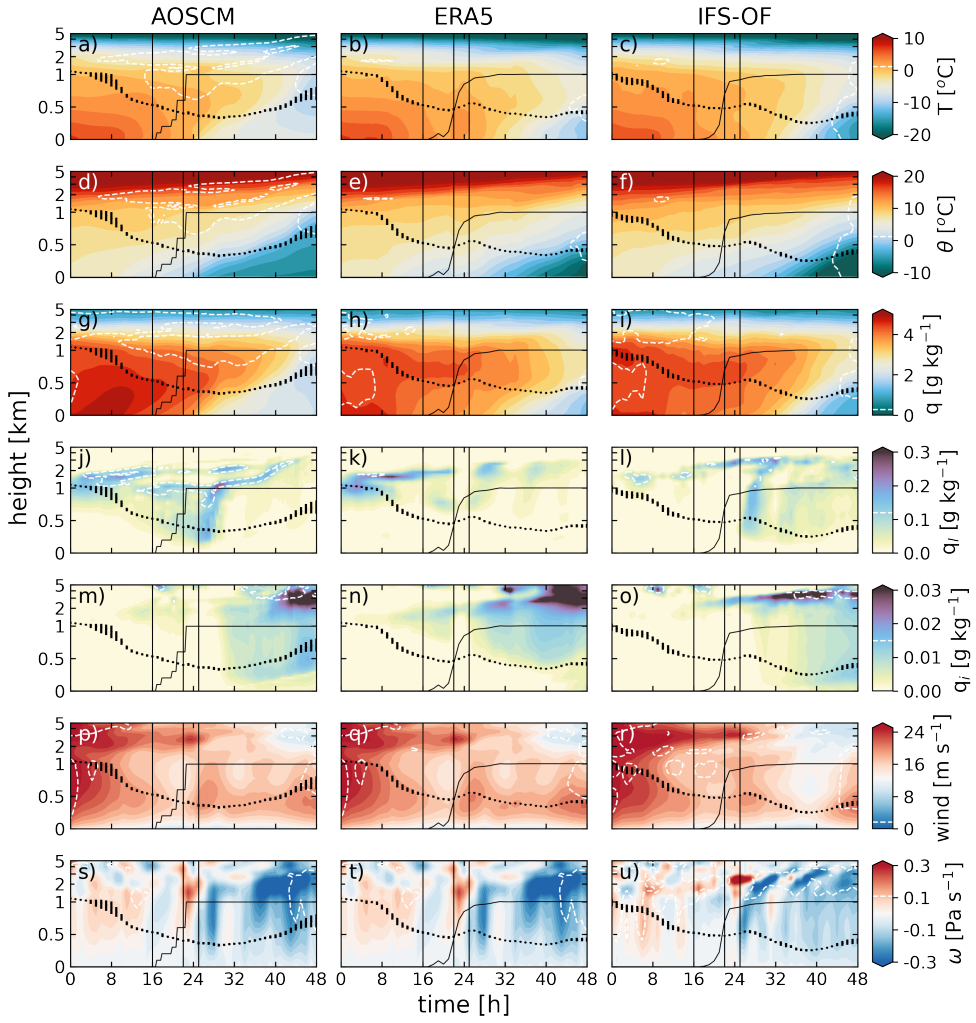

Figure AR1.5: Same as Fig. 5 in the manuscript but with thicker contours for ensemble uncertainty.

- L366–368: So are the ERA5 and IFS-OF representation of the boundary considered more reliable than the AOSCM?

A: Not necessarily. Sea-ice representation varies among the models we are considering in this study. The AOSCM resolves both sea-ice and snow properties and, in that sense, provides a more realistic boundary than ERA5 and IFS-OF in which sea-ice thickness is fixed to 1.5 m and the presence of snow is not taken into account. However, in our Lagrangian application, we divide the trajectories

into smaller legs according to the sea-ice conditions and run consecutive simulations. In general, this helps the AOSCM reproduce important features of the airmass transformation, such changes in heat, moisture and cloud content and overall thermodynamic structure, but may affect the timing of others, especially close to the surface, such as the boundary layer evolution.

- L372: I think the reference to Fig. 5h is actually referring to Fig. 5k,h here? Please also check the other figure references in this paragraph (e.g. reference to Fig. 5i on L374).

A: The references are now pointing to the correct plots.

- L376: To my eye, it looks like the IFS-OF mostly shows a single-layer cloud structure for about 75% of the MIZ and early sea-ice leg.

A: It is true that the appearance of the low-level cloud is somewhat delayed in IFS-OF. The extent of the MIZ is smaller in IFS-OF which could be responsible for the delayed appearance of the low-level cloud. The multi-layer cloud structure is more prominent a few hours later and appears to be linked to the near-surface turbulent cooling the airmass experiences when advected over sea-ice.

- Fig. 6: I don't see several features on this figure that are described in the text. For example, where does AOSCM simulate a drop in temperature below freezing levels (L394–395)? L395 states that dropsondes released over full sea-ice cover show minor surface cooling, but it looks the dropsonde observations are within the envelope of the other temperature profiles in panel (k)?

A: Thank you for pointing this out. The drop below freezing levels does not occur for the AOSCM profile until over the "ice" leg. We rewrite this section to present the results more clearly:

L416-422: "Over the MIZ, the observed air temperature near the surface is slightly positive, approaching zero, which is consistent with the AOSCM, as well as ERA5 and IFS-OF (Fig. 6f). Dropsondes released over full sea-ice cover**, demonstrate a smaller surface cooling compared to the AOSCM ensemble mean (Fig. 6k). In the AOSCM, the near-surface temperature and specific humidity drop by approximately 4 °C and 1 g kg^{-1} respectively (Fig. 6k,l), as a response to the enforced decrease in skin temperature (see Table 1 and Fig. B1). ERA5 and especially IFS-OF match the observed thermodynamic structure near the surface while all products (including the AOSCM) are in agreement with observations over 500 m.** ~~The AOSCM seems to be more responsive to the advection over the sea-ice, showing a more dramatic reduction of temperature near the surface compared to the observations, ERA5 and IFS-OF (Fig. 6k,l)~~**"**

Note that the profiles Fig. 6 have been updated according to our new simulations in which the MIZ is now defined as the region with $0.15 \leq$ sea-ice concentration < 0.8, motivated by comments made by Referee #2.

- Fig. 6: Unless I am missing something, I don't see where the cloud liquid comparisons (right column) are addressed in the text.

A: We have now included a more elaborate discussion on the cloud liquid water profiles. In addition, we have rearranged the order of the subplots in Fig. AR1.6 (Fig. 6 in the manuscript) to enhance the flow of the discussion.

L428-436: "The airmass stratification remains strong over all surface types as demonstrated by the virtual potential temperature profiles, θ_v (Fig. 6c,~~f,g~~h,m). ~~Observations over ocean and, more so, the MIZ show small inversions within the first 2 km (Fig. 6f,g).~~ **Near the surface, agreement with the AOSCM is strong, except for over ice, where the simulated inversion appears much deeper, possibly due to the quick adjustment of the column to the more compact, colder sea-ice surface.**

The AOSCM specific liquid cloud content shows an increase near the surface as the airmass is advected from the ocean (Fig. 6d) to the MIZ (Fig. 6i), indicating the formation of a secondary cloud layer that becomes even more prominent over fuller sea-ice (Fig. 6n). Cloud profile measurements were not conducted during these research flights. However, the observed thermodynamic profiles over ocean and, more so, the MIZ **and sea ice** show small inversions within the first 2 km (Fig. 6h,m). These inversions possibly correspond to a multi-layer cloud structure that agrees with our AOSCM simulations, as well as ERA5 and IFS-OF (Fig. 6~~j~~i-n)**."**

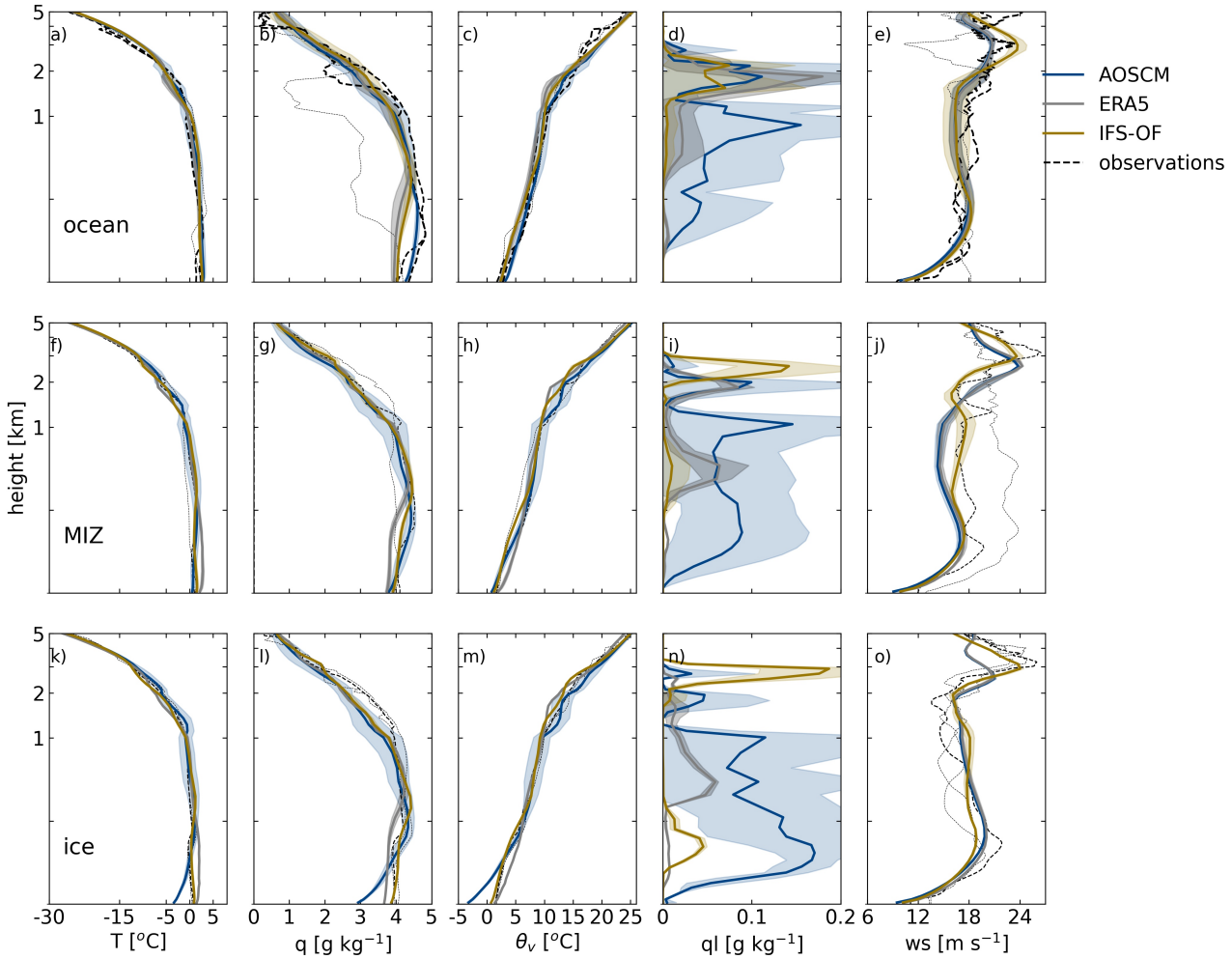

Figure AR1.6: Vertical profiles of temperature (°C), specific humidity (g kg^{-1}), potential temperature, **specific cloud liquid water content (g kg^{-1})** and wind speed **(m s^{-1})** ~~and specific cloud liquid water content (g kg−1)~~ over the ocean(a-e), MIZ(f-j) and sea ice(k-o). Observations are shown with black dashed lines; their thickness represents their proximity to the AOSCM (blue), ERA5 (gray) and IFS-OF (gold) reference profiles for each surface type. The reference profiles were taken close to the majority of the observations (over or around the MIZ) and are denoted with black vertical lines in Fig. 5. The height axis is linear below 1 km and logarithmic above.

- L414–416: It sounds like it would be more accurate to call it the "liquid cloud layer" rather than the "cloud layer".

A: We added “liquid” in all instances where the cloud layer is referenced.

- Fig. 7: The caption does not describe panels e–g. Please check that all figure captions describe the figures in sufficient detail.

A: Panels e-g are now properly described in the caption.

We are also grateful for Referee #1’s technical corrections and for considerable amount of effort and attention to detail they dedicated to reviewing this manuscript. We have applied all of the edits listed below in the new version of the manuscript.

Technical corrections

- L3: "is" --> "are"

- L9: I think "simulate" or "reproduce" would be a better word choice than "emulate" here
- L26: Remove comma after "As"

- L42: "Airborn" --> "Airborne"

- L58: "imporant" --> "important"

- L68: "on" --> "to"

- L134: Add the word "are" after "tracks"

- L197: "dropping" --> "decreasing"

- L211: "air mass" --> "airmass" (to be consistent with the use of this word throughout the manuscript, I would argue that "air mass" is more commonly used in the literature but will leave it up to the authors whether they wish to change it throughout the manuscript)

- L216: Space needed in "of the"

- L293: "big" --> "large"

- L303: "uncertainty range ERA5 and IFS-OF curves" --> "uncertainty range of the ERA5 and IFS-OF curves" (?)

- L305: "and" --> "an"

- L307: "heat-to-moisture" --> "heat-to-moisture ratio" (?)

- L345: "while" --> "with" (?)

- L369: "dropping" --> "decreasing"

- L374: "bares" --> "bears"

- L391: "profiles" --> "profiles are" (?)

Referee #2

The paper investigates air mass transformations (radiative, turbulent, clouds, precipitation) associated with Arctic warm air intrusions. The paper is very well written, with a clear and concise introduction highlighting the existing knowledge and gaps in understanding cloud processes and air mass transformations, and presenting important results which advance our understanding of processes associated with warm air intrusions strongly affecting the Arctic climate. My major recommendations are to strengthen the abstract including key conclusions and slightly modify the results section structure to bring forward the air mass transformation processes and drivers, shifting the focus from model intercomparison. Also, the methodology section requires more details about

the three models used in the study including relevant parameterizations. Below I provide more details. These are relatively minor revisions to clarify certain interpretations and to strengthen the presentation of the paper. I recommend the paper publication after they are addressed.

We are grateful for the reviewer's positive review and valuable input. Their thorough comments helped enhance the quality of the manuscript considerably.

Abstract: The abstract includes detailed methodology description and however lacking somewhat the main results. It will be beneficial for the paper if the readers could learn from the abstract what are the key conclusions regarding the air mass transformation.

A: Thank you for this comment. We modified the abstract to more clearly feature they key findings of the study by adding the following lines.

L9-12: " Cloud radiative cooling and turbulent mixing in the stably stratified boundary layer are constant sinks of heat throughout the airmass transformation. Boundary layer cooling intensifies over the marginal ice zone and forces the development of a low-level cloud underneath the advected one. As the airmass flows past the marginal ice zone, large-scale updrafts dominate the temperature and moisture changes through adiabatic cooling and condensation. "

Data and Methods section: overall it is very clear and well written however some key details regarding observations and models used in the study are missing. In particular:

2.1 Observations: it will be helpful to know more details about the dropsondes (which type, parameters measured directly, vertical resolution, accuracy, etc)

A: Vaisala RD41 dropsondes were used for measuring Temperature, pressure, relative humidty and horizontal wind speed. We specify the dropsonde model in the text and refer to the Vaisala, 2020 datasheet and the HALO-AC3 data overview paper by Ehrlich et al. (2025) for all the relevant technical information. We added:

L87: "equipped with an extensive set of instruments (Ehrlich et al., 2025)"

L89 - 90: "Vaisala RD41 dropsondes **(Vaisala, 2020)"**

L91: "Detailed information on the dropsonde data can be found in Ehrlich et al. (2025)."

2.4 Model description: key details are missing and will be helpful to include in the model description: resolution (ERA5 and IFS), cloud parameterization schemes, convection parameterization, and the snow pack model – in particular, details on how snow on sea ice is represented in the AOSCM.

A: We have added the following lines to

L143-144 "The parameterization schemes for radiation, turbulence, convection and cloud microphysics are described in detail in the IFS cy43r3 documentation (ECMWF, 2017) "

L145-147 "In our set-up, five thickness categories and two vertical levels are used to describe the sea-ice layer while snow is represented by a singular layer on top of the sea-ice. The LIM3 halo-thermodynamic parameterizations are solved for all categories and levels"

Figure 1 caption: "Isobars between 940 hPa and 1080 hPa are plotted with thin(thick) white lines with a 5(10) hPa step" – while it is obvious from the values, it has to be noted that this is mean sea level pressure. Also, including selected makers on the plots will help

A: We have now specified the use of mean sea level pressure in the figure caption. We find that adding the values on the contours, unfortunately, makes the figure less readable without necessarily adding much valuable information. The configuration of the systems that formed the meridional advection corridor is more relevant than their individual strengths for the subject of this study. We made the contours thicker to enhance readability. The MIZ borders have been redrawn to match the new definition, inspired by the referee's next comment.

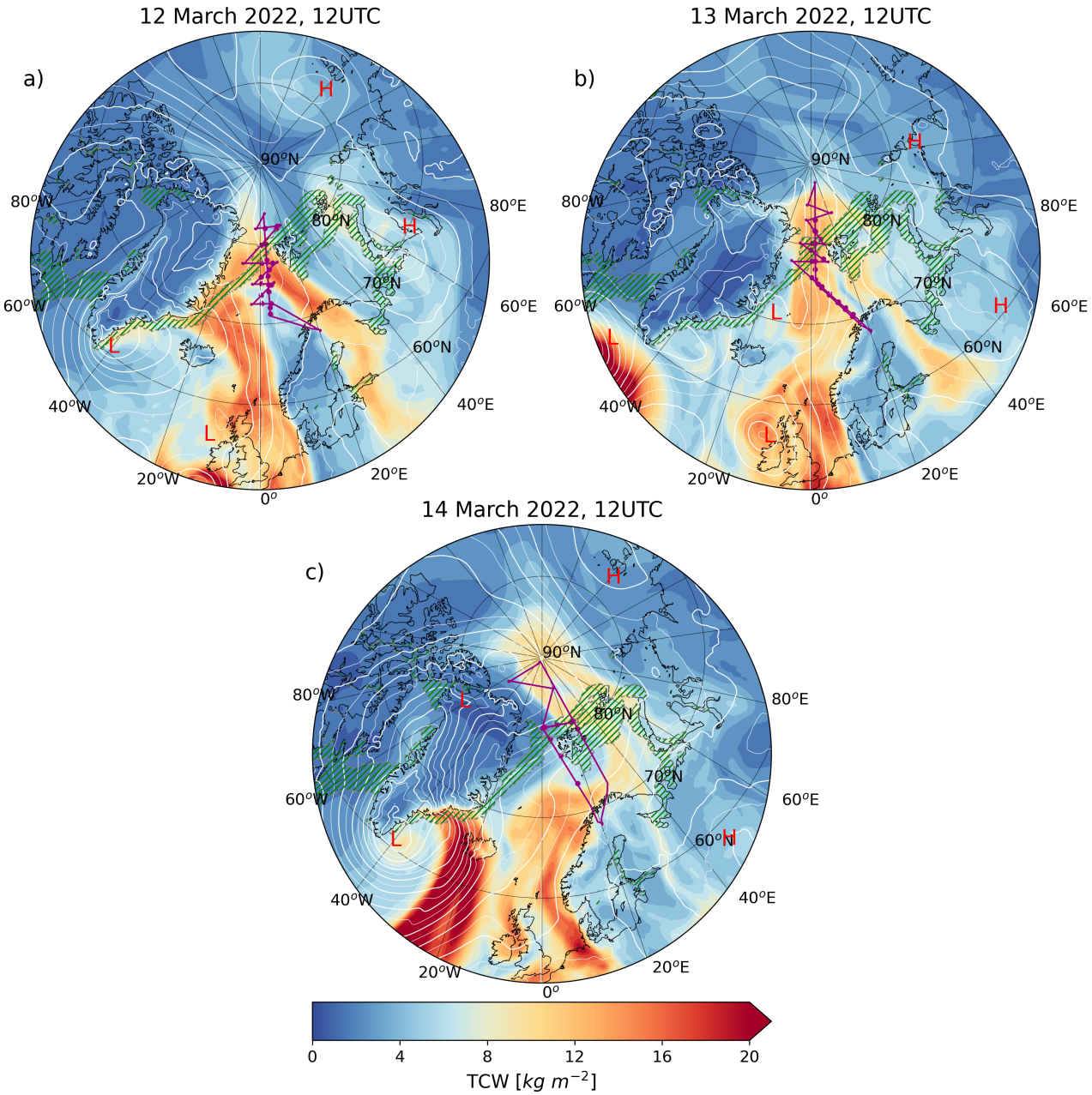

Figure AR2.1: Maps of total column water (kg m–2) at 12 UTC, on each day of the 12-14 March WAI event. **Mean sea level pressure contours** ~~Isobars~~ between 940 hPa and 1080 hPa are plotted with thin(thick) white lines with a 5(10) hPa step. The centers of low and high pressure centers are marked with denoted with red letters. The green hatched area marks the extent of the marginal ice zone (MIZ) which corresponds to sea-ice fraction between values of ~~0~~**0.15** and ~~0.9~~**0.8**. Purple lines represent the respective HALO flight tracks (RF02, RF03, RF04) over the North Atlantic. The purple dots correspond to the locations of dropsondes released during each flight.

Marginal sea ice zone: typically SIC of 80% is used as the upper limit to define MIZ, while the authors used here 90%. Could the authors justify their choice?

A: The definition of the marginal ice zone (MIZ) in our experiments determines the residence time over each surface as well as the representative values for sea-ice concentration and sea-ice and snow thickness of each leg. We initially chose to extend our marginal ice zone (MIZ) definition to include

sea-ice concentrations of 90%, in an effort to account for the contribution of the open water areas more properly.

However, in order to ensure consistency with previous studies and support the broader use of the Lagrangian AOSCM on warm-air intrusion cases in the future, we have redefined the MIZ as the region with 0.15 < sea-ice concentration < 0.8 in our experiments. This change shortens the MIZ leg by approximately three hours. Repeating the simulations with this updated definition produces only minor differences in the overall airmass transformation (Fig. AR2.2). We have now updated all figures and relevant text accordingly.

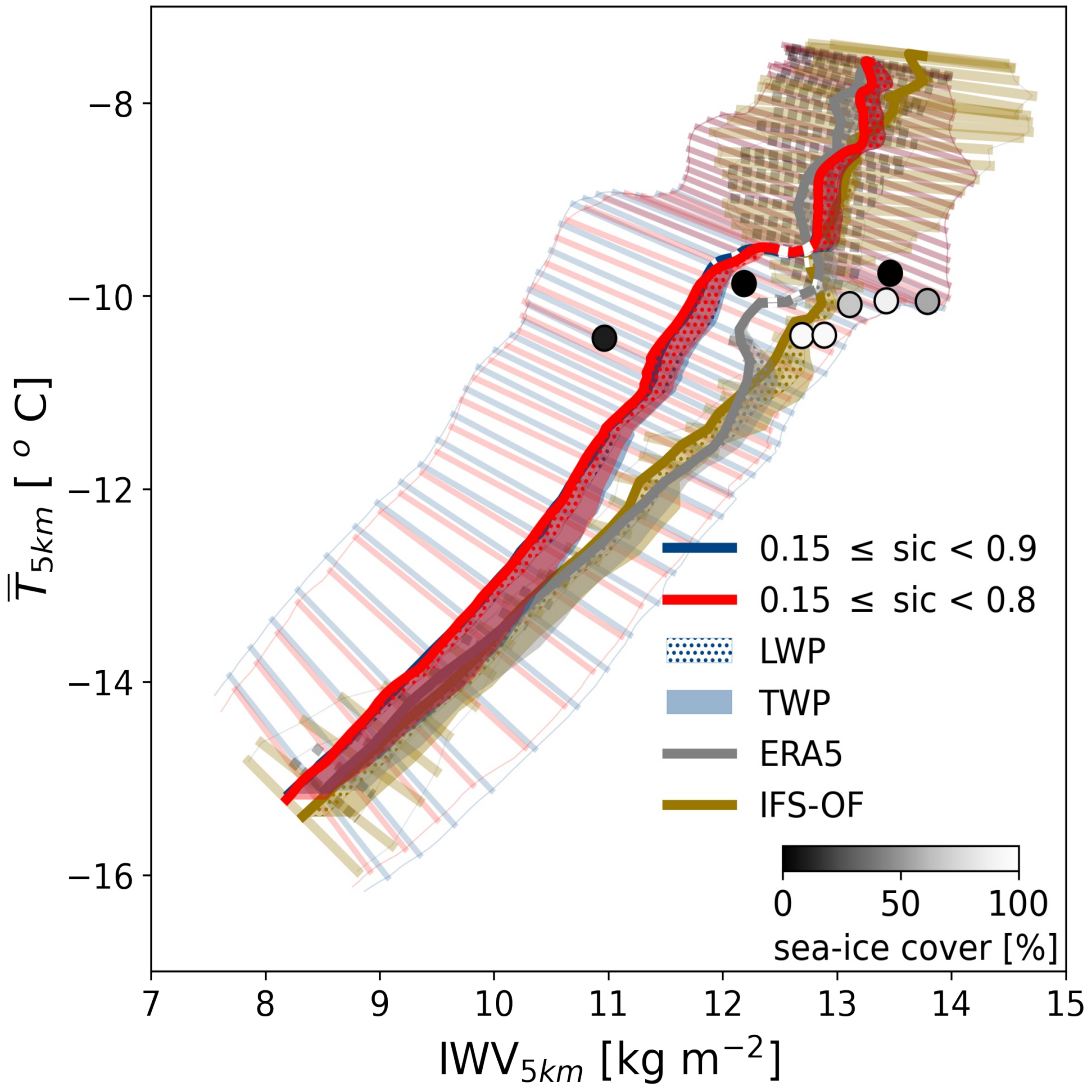

Figure AR2.2: Same as Fig. 4 in the main manuscript but including experiments with different definitions of the MIZ.

Lines 93-94: “On March 13, at 12 UTC we launch 24-hour long trajectories, 600 in total, half of which were computed backward and half forward in time. “ – it will be helpful to show on the figure from where the trajectories launched on Fig. 2a (eg, can highlight in bold the 81ºN line portion near the appropriate meridian not to clutter the figure)

A: Thank you for the suggestion. We added a thick line in Fig. 2 along the 81ºN zone to show the latitude of initialization. We reconfigured and enlarged the plots as proposed by Ref #3.

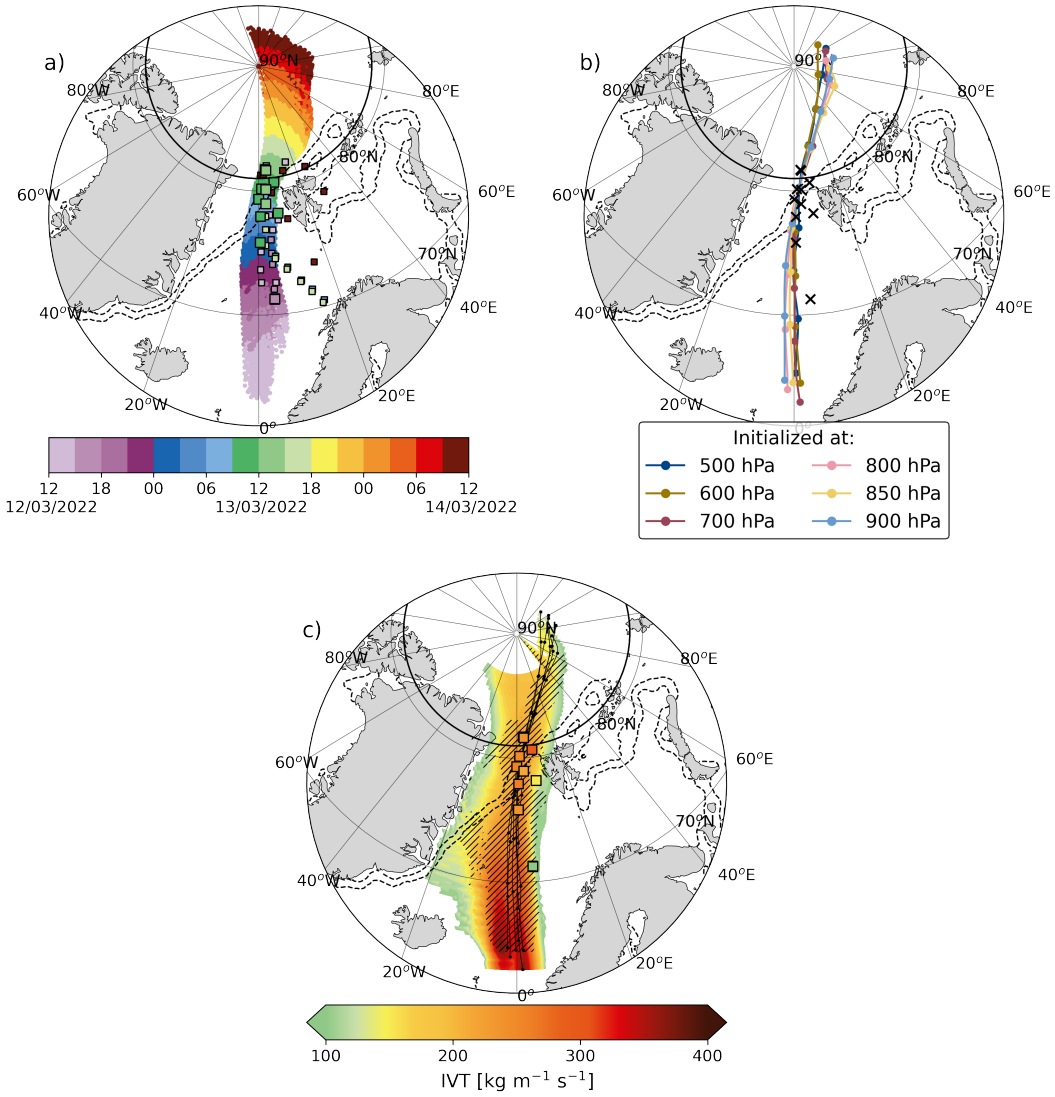

Figure AR2.3: Same as Fig. 2 in the main manuscript.

In the caption, we added the line **"(marked with a thick solid line)"** beside 81° N. We also removed ~~(day of year = 72.5)~~ since it is an unnecessary detail.

Fig 2 c) temporal evolution and spatial variability of integrated water vapor transport (IVT).

Could the authors explain in more detail how IVT temporal evolution is calculated – is it the value for each specific trajectory (which would be difficult given the number of trajectories), along latitudinal line across the trajectory ensemble? Also for trajectories at which level?

A: The trajectories in these plots serve the purpose of a time axis. The trajectory ensemble that we use throughout this study consists of 6 trajectories initialized at 500, 600, 700, 800, 850 and 850 hPa respectively. We follow along each trajectory from south to north and, at each timestep, scan in the perpendicular direction for IVT values of 100 kg m^{-2} s^{-1}, which is a threshold used for Arctic warm-

air intrusion and atmospheric river detection. We repeat the process for all trajectories and present the averaged fields. When examining IVT from this Lagrangian perspective, one can see the width of the airmass and IVT variability in the direction normal to the trajectories and how it evolves in time along the trajectory ensemble.

We rewrote the caption of Fig. 2 to make the method clearer. The new caption is presented below:

"a) 24-hour long backward and forward trajectories initialized at pressure levels (500, 600, 700, 800, 850 and 900 hPa), within a 100 km-radius circle centered on 81 ºN (marked with a thick solid line) and 5 ºE on 13 March, at 12 UTC. The coloring along the trajectories represents the air-parcels' time of arrival at the marked location. The squares mark the locations of all dropsondes released during flights RF02, RF03 and RF04 and are tinted, similarly to the trajectories, according to the dropsonde launch. Smaller squares are used to denote observations whose location and time of launch constitutes the unfit for comparison with trajectories. Dashed contours show boundaries of the MIZ, corresponding to sea-ice concentration values ~~0~~ **0.15** and ~~0.9~~ **0.8**, at the time of the trajectory initialization. **b)** ~~The trajectory ensemble consisting of one trajectory per pressure level, colored accordingly.~~ **The trajectory ensemble showing the closest vertical alignment. Trajectories are colored according to the pressure they were initialized at.** Dots mark 6 hour long periods. X-shaped markers show the locations of observed profiles suited for comparison. **c)** ~~temporal evolution and spatial variability of integrated water vapor transport (IVT). The trajectory ensemble is shown with black lines. Hatches mark the correlation range (see Sect. 2.3) around the airmass at each timestep.~~ **Map of the temporal evolution and spatial variability of integrated water vapor transport (IVT). The trajectory ensemble, drawn with black lines, serves the purpose of a time axis. IVT changes in the direction parallel to the trajectories show the temporal evolution of the airmass. IVT changes in the direction perpendicular to the trajectories show the spatial variability of the airmass at the respective timestep (12/03/2022 12 UTC at the southernmost point to 14/03/2022 12 UTC at the northernmost). Hatches mark the correlation range showing areas around the trajectories of similar vertical structure at each timestep (see Sect. 2.3). "**

We use the same visualization approach for Fig. 3. We make the following changes in the caption of that figure:

"~~The trajectory ensemble is shown with black lines.~~ **The trajectory ensemble, drawn with black lines, serves the purpose of a time axis, similar to Fig. 2c"**

Lines 106-107: "These are identified using an integrated vapor transport (IVT) threshold of 100 kg m−1 s−1, generally preferred for Arctic WAI and AR detection " – I suggest adding also an Arctic-focused paper, eg Viceto et al (2022), and a polar-focused reference by Zhang et al (2024) where specific thresholds are mentioned:

Viceto et al: Atmospheric rivers and associated precipitation patterns during the ACLOUD and PASCAL campaigns near Svalbard (May–June 2017): case studies using observations, reanalyses,

and a regional climate model, Atmos. Chem. Phys., 22, 441–463, https://doi.org/10.5194/acp-22-441-2022, 2022.

Zhang et al: Extending the Center for Western Weather and Water Extremes (CW3E) atmospheric river scale to the polar regions, The Cryosphere, 18, 5239–5258, https://doi.org/10.5194/tc-18-5239-2024, 2024.

A: Thank you, we have now cited the suggested studies.

L125-126: "; Viceto et al., 2022; Zhang et al., 2024"

Lines 145-150: "The presence of snow on ice, not allowed in OpenIFS, has also been shown to mitigate surface energy and near-surface air-temperature biases (Pithan et al., 2016). " – it is not clear how the presence of snow on ice is treated in the AOSCM – please include more details as this is an important parameter influencing surface fluxes (especially the surface albedo and netSW). Is it from observations or parameterized?

A: Snow thickness is initialized according to CMEMS reanalysis data. Initial values for snow thickness and other sea-ice properties are now given in Table 1 in the main manuscript. As stated above, the sea-ice layer is described by 2 vertical levels and 5 thickness categories while snow is represented by a singular layer on top of the sea-ice (**L145-147) .** The LIM3 halo-thermodynamic parameterizations are solved for all categories and levels. For more information on the sea ice model physics, we refer the reader to the LIM3 documentation ((Rousset et al., 2015).

The simulated surface albedo is, on average, 0.56 for the MIZ and 0.93 for the sea-ice region, which is reasonable considering the respective sea-ice concentrations of approximately 0.6 and 0.99. We note that, in mid March when our WAI of interest is taking place, the amount of solar radiation reaching the snow surface is relatively small. Therefore, net SW does not influence the surface energy budget immensely. Turbulent heat fluxes (sensible and latent), as well as the downwelling longwave radiation are much stronger contributors. The sensible and latent heat fluxes are computed according to the surface skin temperature which we keep constant in time by initializing the sea-ice and snow layers with larger heat contents (colder temperature values).

"

Table 1. Representative values for sea-ice and snow properties used in the coupled simulations.

	MIZ	ice
Sea-ice concentration	60 %	99 %
Ice thickness	0.90 m	2.1 m
Snow thickness	0.13 m	0.31 m
Skin temperature	~ -1.5 ºC	~ -8 ºC

"

Fig 3: For the flux plots, it should be indicated in the caption that the flux is positive towards the surface. For SW and LW fluxes – please specify in the caption that these are net fluxes.

A: Thank you, we added the sign convention for the fluxes in the caption. Fig. 3 caption: **"Fluxes are positive towards the surface."**

Fig 3 caption: "in terms of integrated specific water content " – suggestion to add "integrated"

A: Fixed.

Line 218: "On the western flank of the airmass, where the LWP is larger, less solar radiation reaches the surface.. " – the statement is not clear. As the plot is showing netSW radiation at the surface, a large impact over the perennial sea ice and MIZ is most probably explained by the high surface albedo and reflection of a large portion of the incoming SW flux. My earlier question – how the snow on sea ice is treated – is an important factor to consider also over the sea ice zones. However, it is not clear why the netSW flux sharply decreases from rather large values south of 70ºN to almost zero north of it and then stays around zero over the open ocean not changing much over sea ice. It will be useful to include also a map of the surface albedo together with downwelling SW and investigate processes controlling netSW in more detail (in the later section using AOSCM). Part of this can be probably explained by changing solar zenith angle however the differences across the 70ºN are too sharp.

A: The area covered by the warm-air intrusion, at the time of the event (March 12-14) receives roughly 7 to 11.4 hours of daylight, at the northernmost and southernmost point of the trajectories respectively. The maps in Figures 2 and 3 show how the different variables evolve in time, along the path of the advection. At 65° N and 12 UTC (which is also local time for the airmass since it is advected along the prime meridian) the surface receives a maximum SW of around 200 W m^{-2}. The airmass then travels 5 latitudinal degrees in 6 hours and reaches 70° N around sunset, when SW at the surface drops to 0. Solar radiation increases again around the MIZ area, but the flux at the surface is significantly smaller due to the zenith angle (~12 W m^{-2}) . We have added explanatory comments to the captions of Figures 2 and 3 to clarify the Lagrangian map visualization method, which should help readers interpret the figures more effectively.

Figures 2 and 3 were produced with ERA5 data. ERA5 is the combined product of IFS cy41r2 and assimilation of observations, including satellite radiance measurement. IFS cy41r2 does not allow snow on sea-ice but representation could be corrected during the assimilation process.

The Lagrangian map of the temporal evolution and spatial variability of albedo is attached below (Fig. AR2.4). Albedo is computed as $Sw_{surf}^{up}/Sw_{surf}^{down}$, therefore the night-time parts during the airmass transport are excluded.

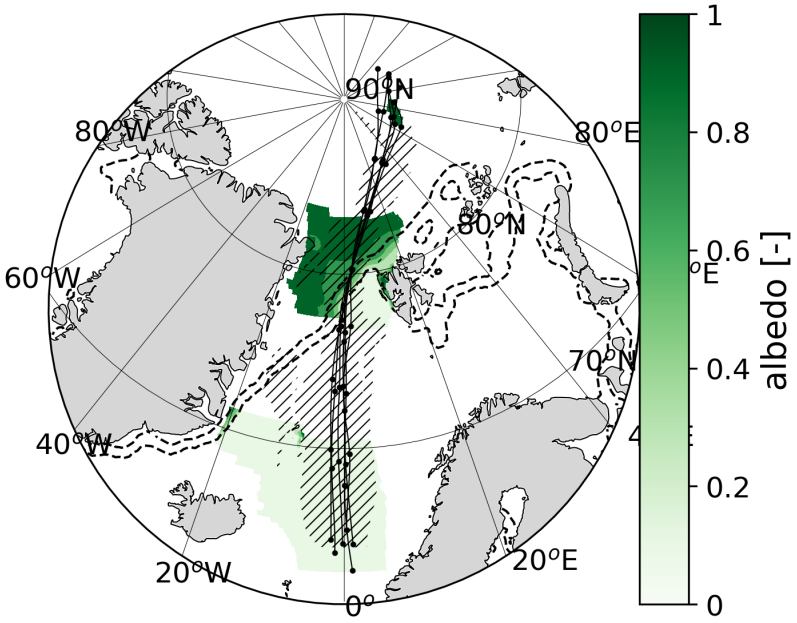

Figure AR2.4: Temporal evolution and spatial variability of the airmass during its poleward advection in terms of albedo. The trajectory ensemble is shown with black lines. Hatches mark the correlation range (see Sect. 2.3) around the airmass at each timestep. Square markers, when present, correspond to the observed values. Dashed contours show boundaries of the MIZ, corresponding to sea-ice concentration values ~~0~~**0.15** and ~~0.9~~**0.8** on March 13, at 12 UTC.

Lines 220-225: “The spatial variability in skin temperature over the ocean also appears to be controlling the exchange of latent heat at the surface (Fig. 3h). Over the warm ocean, the strongly negative (upward) fluxes indicate the ongoing moisture uptake by the airmass. “ : can you please clarify your interpretation. The upward LH flux indicates surface evaporation, which indeed seems to be related to the skin T according to the plots, while it is also strongly controlled by the near-surface winds and the boundary layer RH. To be sure that this evaporated moisture is taken by the air mass needs verification if the trajectory was within the boundary layer. Was this the case over the region with surface evaporation? It is anticipated that these questions are considered further when using AOSCM. Then the limitations of using ERA5 shall be stated clearly also highlighting the added value of modeling investigations. Boundary layer height is later shown in the AOSCM (Fig. 5) however the two sections (3.2 and 3.3.4) are somewhat disconnected.

See for example:

Sodemann, H.: The Lagrangian moisture source and transport diagnostic WaterSip V3.2, EGUsphere [preprint], https://doi.org/10.5194/egusphere-2025-574, 2025.

Sodemann, H., & Stohl, A. (2009). Asymmetries in the moisture origin of Antarctic precipitation. *Geophysical Research Letters*, **36**(22). **https://doi.org/10.1029/2009GL040242**

A: The lowest trajectory of the ensemble is within the boundary layer for the first 8 hours when surface evaporation is on-going. Therefore, this is a process that is relevant for this airmass transformation. Our modeling framework views the airmass as a a cohesive air column that is advected uniformly within the lowest 5 km, which makes the interaction with the surface relevant through the entire transformation, regardless of the position of the trajectories relative to the boundary layer top. We highlight the advantages of this modeling approach in the Introduction.

L75-76: "In this simple, novel framework we can investigate the physical drivers and timescales of the transformation, in isolation from the complex dynamics that are typically associated with warm-air intrusions."

Further downstream the boundary layer becomes shallower and the airmass is lifted by a large-scale updraft, becoming progressively more decoupled from the surface (Fig. AR2.5). In reality when that happens, low-level convergence should bring new airmasses into the column through horizontal advection, which is something that our modeling framework does not take into account. This is already discussed as a limitation to the Lagrangian AOSCM but will be stated more clearly in the conclusions.

L538-539: "It is important to note that the large-scale updrafts applied in our simulations would normally be accompanied by low-level convergence and, therefore, advection of new air in the column which is prohibited in our framework."

We plan to explore the importance of the complex dynamic conditions during warm-air intrusions (WAIs) in greater detail in future work using this Lagrangian modeling framework.

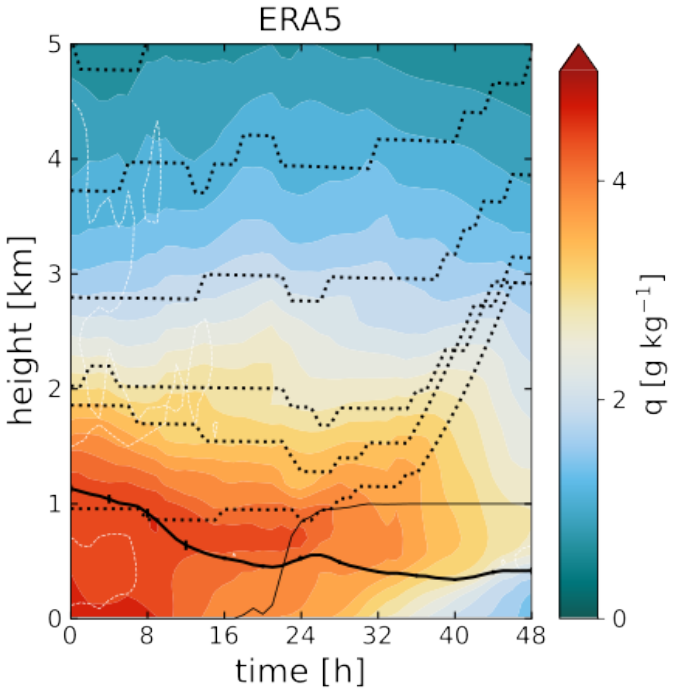

Figure AR2.5: Time-height cross-sections of the ensemble average specific humidity from ERA5. Dotted lines represent the height of the trajectories. The thick solid line shows the evolution of the

boundary layer height during the airmass transformation. The thin solid line marks the along-stream sea-ice concentration.

Section 3.3.3: I suggest including a reference to Fig. 4 to make it clear the results are based on this figure

A: Added figure reference in **L317**.

Lines 300-305: "The uncertainty range ERA5 and IFS-OF curves grows larger due to the slight divergence of the trajectory ensemble. " – I am not sure to follow this interpretation. My understanding from reading the methodology is that the trajectories are the same, while thermodynamics state is represented by 3 different models (ERA5, IFS-OF and AOSCM). Thus, this is not the divergence of the trajectory ensemble but shall be explained by the differences in the model physics and processes representation. Could you please clarify and rephrase the statement.

A: We apologize for the confusing phrasing here. With the term "uncertainty range" we do not refer to the differences between ERA5 and IFS-OF which, as the reviewer points out, would be the result of differences in model physics and assimilation of observations. "Uncertainty range" in Fig. 4 are the perpendicular faded line that show the variability in the thermodynamic state within the trajectory ensemble in each dataset. For ERA5 and IFS-OF that range shrinks around the MIZ over which the trajectories were initialized and their in-between distances are the smallest. As the trajectories spread out towards the northernmost and southernmost end, they span a larger area and captures more of the airmass variability making the uncertainty range around the ensemble mean grow.

We rephrase:

L325: "~~The uncertainty range ERA5 and IFS-OF curves grows larger~~ The uncertainty ranges around the ERA5 and IFS-OF curves grow larger"

Fig 5: Please indicate the time 0 (2/03/2022, 00UTC) in the caption

A: Added **"The time axis is in hours since 12/03/2022, 12UTC."** in the caption.

Line 355: "Over the MIZ, the subsidence spikes abruptly and over the sea-ice leg the vertical motion is predominantly upward, with ω increasing the deeper the airmass intrudes into the Arctic. ": is this updraft driven by cloud top radiative cooling (as described in Morrison et al 2012)? This can be seen in Fig. 7a discussed later in section 3.3.6.

Morrison, H., de Boer, G., Feingold, G. *et al*. Resilience of persistent Arctic mixed-phase clouds. *Nature Geosci* **5**, 11–17 (2012). https://doi.org/10.1038/ngeo1332

A: The AOSCM is forced with ERA5 vertical velocities (ω) shown in Fig. 5 (s-t) in the main manuscript. Therefore, these updrafts represent large-scale motions that can not be resolved in the single-column format and are therefore prescribed. In order to isolate the cloud ascent caused by the

model physics we would need to deactivate vertical advection (Fig. AR2.6). The ascent of the top cloud layer is much slower and, in the absence of adiabatic cooling, weaker changes in the heat and moisture content of the airmass in total. This is an interesting aspect of the transformation and, although it is outside of the scope of this study, we plan to investigate it further in our future Lagrangian AOSCM applications.

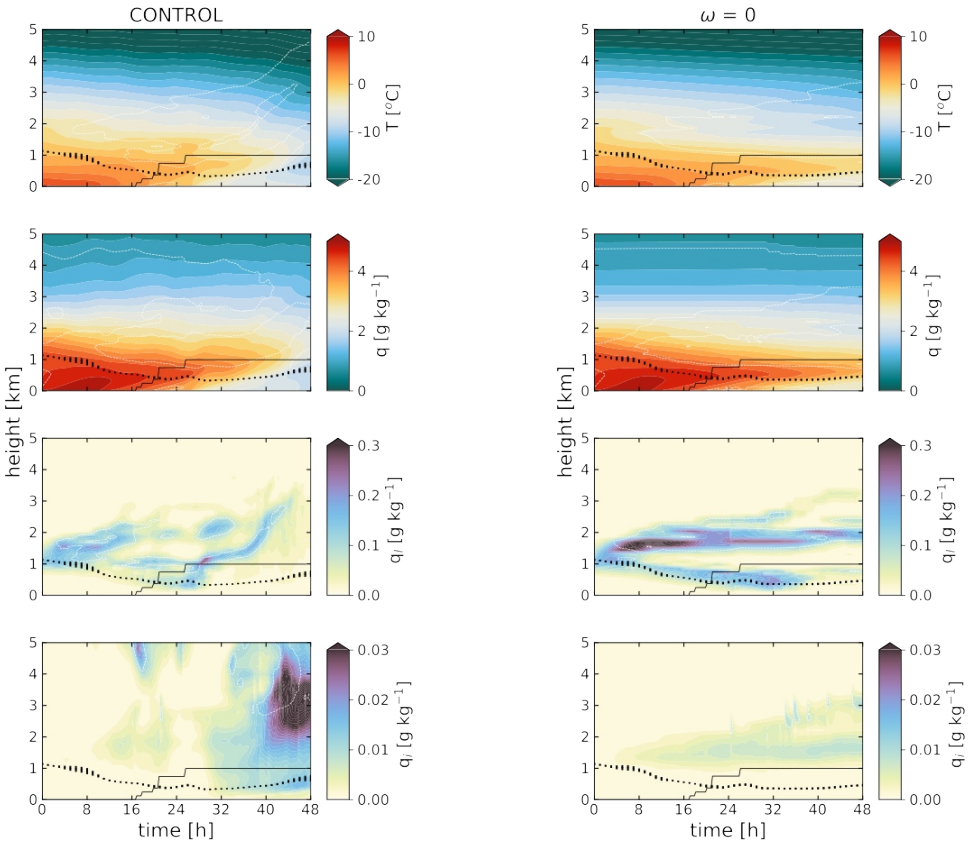

Figure AR2.6: Time-height cross-sections of the ensemble average temperature (1st row from the top), specific humidity (2nd row), specific liquid (3rd row) and ice water (4th row). The left column shows the AOSCM simulations as presented in the manuscript and the right column shows experiments with vertical advection switched off (ω = 0).

To make more emphasis on the process understanding I suggest to move section 3.3.5 "Comparison with observed transformation" before section 3.3.4 – this will show how each model represents each parameter before investigating the evolution in these parameters. Further, it will be beneficial to combine sections 3.3.4 "Vertical structure" with section 3.3.6 "Physical and dynamical drivers" explaining the drivers (Fig. 7) right away when presenting the vertical structure transformations (Fig. 5).

A: We think the discussion of vertical structure Sect. 3.3.4 is a more natural continuation of Sections 3.3.[1-3] that describe the transformation in bulk terms. Sect. 3.3.5 then focuses on the smaller areas of the cross-sections where observations are available. It is, in our opinion, preferable to present the airmass transformation in its entirety before focusing on the specific points where observations are available.

Section 3.3.5: As cloud ice and liquid content are key drivers of the radiative fluxes and updrafts, can the authors also include cloud evaluation, eg with cloud LWP from HAMP onboard HALO? I understand that this can be beyond the scope of the paper but if the data are already available this will be beneficial to see how AOSCM represents cloud properties.

A: Thank you for raising this point. LWP retrievals from HAMP were still a work in progress when this manuscript was submitted but are now available. We are pleased at the opportunity to include them in our plots. We have incorporated the observed LWP values in AR2.7 (Fig 3b in the manuscript).

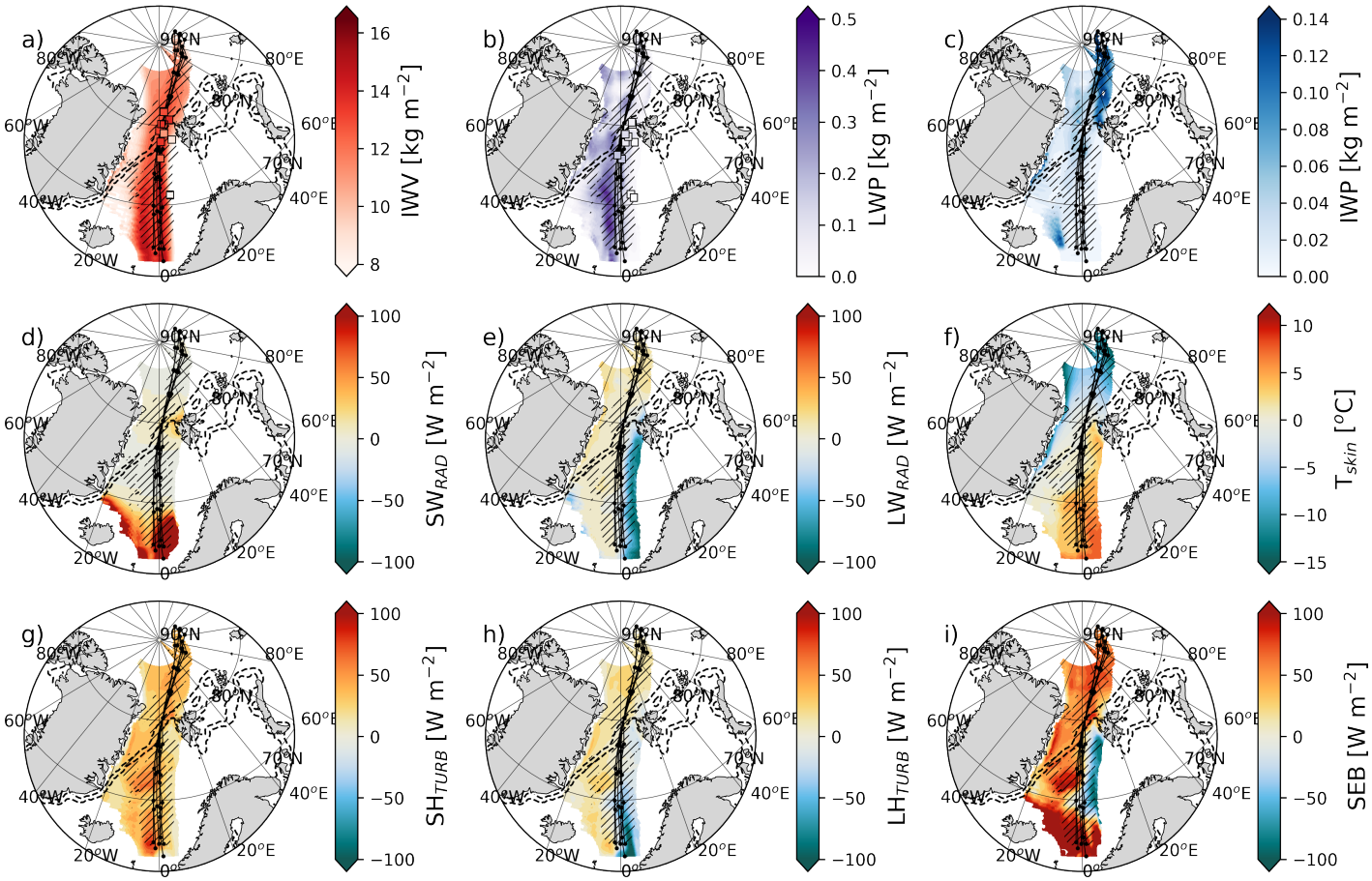

Figure AR2.7: Same as Fig. 3 but with LWP retrievals based on HAMP observations included in Fig. 3b.

We offer a description of the dataset in Sect. 2.1 and discuss the results in:

L238-241: "The observed spatiotemporal cloud distribution is similar to ERA5. ERA5 shows a positive LWP bias (-0.03 kg m^{-2} on average) in the east sector of the airmass, where the cloud is thin, and a negative LWP bias (-0.04 kg m^{-2} on average) in the west where thicker clouds are encountered. The biases are larger than estimated uncertainty of the LWP retrieval (0.02 kg m^{-2})."

Minor edits:

Line 168 : "of a strong cyclone" - add 'a'

A: Fixed.

Throughout the text – spaces missing at multiple places

A: We skimmed the text and added missing spaces.

Referee #3

Summary

Karalis et al. aim to enhance the understanding of airmass transformation occurring during warm air intrusions (WAI) in the Arctic. They propose a new single-column Lagrangian framework for simulating realistic WAI events and justify this by their findings that the WAI behaves as a column in the atmosphere. A case study of a WAI from 12-14 March is used to evaluate the performance of their framework, in which they do a comparison against dropsonde measurements, ERA5 and IFS forecast data. By looking at heat, moisture content and the vertical thermodynamic and cloud structure they conclude that the model adequately reproduces the transformation. They state the value of the model as a source for identifying common features between airmass transformations and for identifying model biases.

The paper presents an interesting study aiming to enhance the understanding of warm air intrusions in the Arctic. My main recommendations revolve around highlighting the novelty and use of your work and clarifying the description of the methodology for this new approach. After these comments have been addressed I think the paper will be a valuable contribution for further work in understanding airmass transformation in the Arctic. Below I attach major and minor comments that hopefully will be useful in preparing a revised version of the manuscript.

We thank the reviewer for their detailed and constructive feedback. Their comments helped us iron out points of ambiguity in how we present our methods and findings and overall benefited the manuscript considerably.

Major comments

3. It was not very obvious from the Introduction how this paper innovates from the plain Lagrangian framework applied in Svensson et al., 2023, even though this becomes somewhat clearer later on in the methods section. The novelty and use of the single-column framework should be better highlighted in the text upfront in the introduction, throughout the results, and in the discussion/conclusions (see comment 2).

A: Thank you for pointing this out. The novel features of this study are

1. the development of a single-column modeling framework capable of simulating realistic warm-air intrusion cases and
2. comparison with observations also conducted from a quasi-Lagrangian perspective.

This may not become clear enough early on. In the new version of the manuscript, the novelty of the method is stressed more in the introduction:

L72-79: "~~The suite of Lagrangian observations available for this case makes it a suitable testbed for the development of a Lagrangian single-column modeling framework to study real WAI cases, as per Pithan et al. (2016, 2018)'s suggestions. We use the Atmosphere-Ocean Single-Column Model (AOSCM, Hartung et al., 2018) to investigate the processes that drive the airmass transformation. We compare our simulations to observations, ERA5 and IFS forecast data in order to assess the performance of the model and its potential as a tool to test and construct future model parameterizaton schemes.~~ **We develop a Lagrangian single-column modeling framework suitable for the study of real WAI cases, as per Pithan et al. (2016, 2018)'s suggestions. We use the Atmosphere-Ocean Single-Column Model (AOSCM, Hartung et al., 2018) and take into account the time-varying dynamic and surface conditions that are relevant for the Arctic airmass transformation. In this simple, novel framework we can investigate the physical drivers and timescales of the transformation, in isolation from the complex dynamics that are typically associated with warm-air intrusions. Through comparison with the large number of Lagrangian HALO-(AC)^3 observations available for this case, as well as ERA5 and IFS forecast data we assess the model's performance and its potential as a tool for testing and developing future model parameterization schemes."**

4. The airmass trajectories for this case are almost entirely north-south oriented. It seems thus that for such straight-line trajectories one could get a lot of the same information from a simple cross-section without running the single-column model in addition. Thus, it is important to highlight what the additional value of this approach is.

A: The aim of our study is to introduce a simple and efficient framework that is suitable for the study of Arctic airmass transformation, not only for this case but for a suite of them. Using our single-column modeling framework to study the airmass transformation has several benefits:

1. It is much faster and less resource-intensive than its 3D counterpart, which facilitates the application of a large number of experiments in a short amount of time.
2. It is able to reproduce the Arctic airmass transformation realistically similarly to the 3D model, as seen through comparison with ERA5, IFS-OF and observations.
3. It is fundamentally Lagrangian. In a time-height cross-sections extracted from Eulerian gridded products (reanalysis or model output) it is harder to distinguish between changes induced by physical processes and the ones caused by advection. In the Lagrangian AOSCM horizontal advection is deactivated and mass is conserved. This helps more clearly demonstrate how the different physical processes affect the airmass evolution.
4. In this framework, the dynamic evolution of the large-scale flow is not resolved, but rather used as input/forcing. The advantage in preserving the flow when testing the effect of different model parameters or parameterization schemes.

These points are established in different sections of the manuscript. We offer a summary in our conclusions:

L543-551: "In conclusion, our Lagrangian AOSCM framework is a novel tool that facilitates the simulation of realistic WAI events and, therefore, the direct evaluation with observations and can virtually be applied to simulate any case of meridional airmass transport. ~~The use of the model on a wide range of warm-air intrusions and cold-air outbreak events that have been captured over time by ship and aircraft campaigns would be a valuable source of information in identifying common features between the respective airmass transformations and uncovering persistent model biases. The AOSCM shares the same physical parameterizations as in EC-Earth and OpenIFS and, according to our results, is able to reconstruct an airmass transformation similar to its global equivalent. A more expansive study using the Lagrangian AOSCM framework could be used for the mitigation of long-standing parameterization deficiencies related to the airmass transformation and consequently the Arctic climate, conducing to a long-term benefit for weather forecasts and climate projections~~. **The AOSCM shares the same physical parameterizations as EC-Earth and OpenIFS and, despite being conceptually simpler and significantly less resource-intensive, it is able to reconstruct an airmass transformation similar to its global counterpart. This makes the model well-suited for wider application to more warm-air intrusion and cold-air outbreak events that have been captured over time by ship and aircraft campaigns. A more expansive study using the Lagrangian AOSCM framework would be valuable for identifying common features among airmass transformations. The model's ability to separate physical processes from the complex dynamics of WAIs can help uncover persistent Arctic-related model biases, mitigate long-standing parameterization deficiencies and eventually improve weather forecasts and climate projections."**

5. The authors make a strong statement in the conclusion about the novelty of this study, but it is difficult to distinguish the contribution here from the works of others, which is discussed both in the conclusion and also to some extent in the results part. In order to make it easier for the reader to follow the argumentation of how these results are novel, a dedicated discussion section would be useful. This would also allow to focus more on the conclusions from this work in the final section.

A: Our results about the vertical coherence of the flow lay the foundation for the application of the Lagrangian AOSCM. Therefore, we think that, in many parts of our manuscript it is essential for the results to be interpreted right away in order to move on to the next chapter. Adding a separate discussion section may increase the length of the paper substantially and lead to unnecessary repetition. We would prefer to not proceed with any major structural changes. However, we can deal with the ambiguities that the reviewer has rightfully pointed out and fix the confusing merging of discussion points and conclusions.

We moved a part of the conclusions to the end of Sect. 3.3.6 "Physical and dynamical drivers" where discussing the effects of subsidence in the context of past research is more appropriate"

L510-517: "The role of subsidence has not been adequately accounted for in the mostly idealized WAI airmass transformation modeling studies that have been attempted to date (Pithan et al., 2018). Part of the reason lies in the lack of observations and/or observational methods for the large-scale vertical motion, making reanalysis products, such as ERA5, the

most common source for forcing information in SCM and LES experiments. The HALO-(AC)^3 campaign (Wendish et al., 2024) attempted measuring the large-scale subsidence on multiple counts (Paulus et al., 2024), including a cold-air outbreak event. Their results showed variable agreement between measurements and ERA5 reanalysis, at times displaying a significant mismatch in the magnitude and even sign of vertical velocity (ω). In this context, it is difficult to determine whether the prescribed subsidence profiles in our simulations and their consequent impact of the airmass transformation are realistic."

In the Conclusions section we replaced the moved text with the following to making it more clear that the paragraph is a summary of the framework's potential limitations:

L537-540: "Furthermore, errors in our simulations may have arisen from the large dependence on the along-track prescribed ERA5 vertical velocity, the accuracy of which is inconsistent (Paulus et al., 2024). It is important to note that the strong updrafts applied in our simulations would normally be accompanied by low-level convergence and, therefore, advection of new air in the column which is prohibited in our framework."

6. The method is not sufficiently clear, in particular when it is being referred to an ensemble. Some additional details on how the trajectories and the ensemble are obtained would be helpful for the interpretation. I suggest to illustrate this with a conceptual figure instead of using a result figure in section 2.2/2.3.

A: We agree that a conceptual figure would be a valuable contribution, however, we have not been able to design such a figure that demonstrates the ensemble in a better way than the concrete example does.

7. Another step in the method that needs further justification is the meridional search for threshold values from trajectory points. It seems odd to go from a Lagrangian framework to a search for threshold values in an Eulerian perspective. Why not use a threshold in a Eulerian map of TCWV directly? When 'stepping outside' the trajectories, there is no more guarantee for that the airflow aligns and goes into the same direction.

A: While it is true that the flow across the WAI may vary, airmasses within a certain distance from the trajectories are shown to move similarly to the ones on the trajectories and, furthermore, experience a similar transformation. This can be seen in Fig. 2c where areas around the trajectories are shown to have similar IVT (integrated water vapor) values and vertical structure. IVT (Fig. 2c) and IWV (integrated water vapor, Fig. 3a) show similar spatiotemporal variability, indicating that the wind field is actually quite coherent around the trajectory ensemble. Further evidence of that can be found in Fig.1 where the MSLP (mean sea-level pressure) contours are roughly equally spaced at the respective location of the airmass at each timestep and Fig. 2a from the narrow and coherent appearance of the larger suite of trajectories.

The Integrated Vapor Transport (IVT) threshold of 100 kg m-2 s-1 is used to estimate the extent of the airmass in the direction perpendicular to the axis of advection. The benefit of visualizing this in a Lagrangian way is:

1. Establishing that the trajectory ensemble is part of a larger airmass that moves and transforms in a coherent way
2. Demonstrating the variability in the transformation of the airmasses beside the one we chose to focus on. This helps determine whether our conclusions about the important processes and timescales of the transformation are tied to this specific airmass or can be considered relevant to the airmass transformation in general under similar conditions.

We explain how this airmass tracking/visualization method helps interpret vertical coherence in the manuscript. We add the following lines in Sect. 3.1:

L214-216 : "~~Therefore, all trajectories within the ensemble can be regarded as representative of the same air column.~~ **In simpler terms, the flow within a certain distance from the trajectories is relatively unirform, both in IVT and vertical structure. Therefore, our trajectory ensemble is narrow enough to be regarded as representative of a single air column that is advected and transformed in a coherent way."**

We have also rewritten the captions of Figures 2 and 3 to ensure the visualization method is clear to the reader.

8. L180: This appears to be a fundamental conclusion to move ahead, but the vertical alignment is not clear from the results. Maybe it could be quantified with a dispersion metric to underline how the trajectories move together? Additionally, a figure showing this result would be helpful, for example showing the vertical position of traced air parcels over time.

A: The trajectories are calculated in latitude - longitude coordinates, so any dispersion metric applied on those would not be particularly meaningful considering the convergence of the meridians as the airmass progresses to the north. Plotting the vertical position of the parcels over time does not necessarily help with evaluating their vertical alignment either (Fig. AR3.1). The closest thing to a dispersion quantifier would be the horizontal spread of the trajectories or, in more specific terms, the distance of the parcels that are the farthest from each other at each timestep. As already stated in the manuscript, the horizontal spread grows from 0 (at the location of initialization) to around 260 km at the two ends of the ensemble. We have now refined the phrasing to ensure the information is clear.

L203-205: "~~Within this large suite of trajectories, smaller subsets can be found, comprised of one trajectory per pressure level, that exhibit a considerably narrower spread, to the point where they appear roughly vertically aligned. The subset closest to observations is pictured in (Fig. 2b), with maximum width around 260 km.~~ **Within this large suite of trajectories, we find a smaller subset, comprised of one trajectory per pressure level. The trajectories in this subset exhibit a considerably narrower spread (260 km at the point of maximum divergence), thus appearing roughly vertically aligned (Fig. 2b)."**

However, that metric alone can not be used to argue whether the trajectory ensemble is narrow enough to resemble the advection of column-like airmass. The analysis about the extent and variability in the WAI, presented in Sect. 3.2, is necessary to confirm that all trajectories belong in the same airmass.

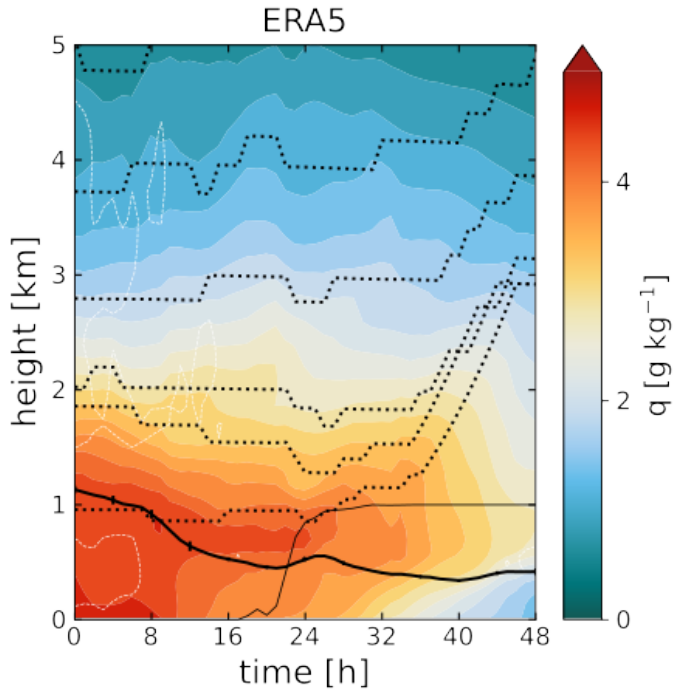

Figure AR3.1: Time-height cross-section of the ensemble average specific humidity from ERA5. Dotted lines represent the height of the trajectories. The thick solid line shows the evolution of the boundary layer height during the airmass transformation. The thin solid line marks the along-stream sea-ice concentration.

9. The title is not sufficiently connected to what is shown in the manuscript, which is a novel model framework illustrated by a single WAI case from a campaign. For that it is not necessary to promote the HALO-(AC)3 campaign in the title. I suggest a title along the lines of: "Lagrangian single-column modeling of Arctic airmass transformation during a major warm air intrusion"

A: We have considered changing the title according the reviewer's suggestion. However, the novelty of the framework partly lies in the availability of quasi-Lagrangian observations that can be used for comparison and model evaluation. Therefore, we believe HALO-(AC)3 should be kept as part of the title.

General comments

Several sentences and parts of the manuscript are hard to read and it is not easy to grasp the flow in a paragraph. This is probably due to interruption of the sentences by references and by a reversed order of the old and new information in sentences (see for example Gopen and Swan,

https://www.americanscientist.org/blog/the-long-view/the-science-of-scientific-writing). See technical comment L214 and minor comment L155 and L156 for examples.

A: We apologize for the awkwardly structured sentences or poor use of language that may have led to unnecessary confusion. It can be challenging for a non-native speaker to describe complex ideas with simple sentences, thus we are grateful for the reviewer's honest feedback. In our effort to address all of the reviewers' comments we have edited a considerable portion of the manuscript, aiming for the best formulation possible in each instance. Considering that the other two anonymous referees described the text as well written, we hope that, through our changes, we have been able to address all major areas of ambiguity.

Figures

Figure 1 is too small, consider using 2 rows and 2 columns instead. The features are hard to distinguish, especially the green on top of the dark blue. The purple dots are nearly invisible.

Figure 2: this figure is also a bit small. The figure caption does not sufficiently make it clear how to understand this figure. This is also connected with the uncertainty of how the trajectories are obtained (see major comments).

A: We have now resized and reconfigured Fig. 1 and Fig. 2 to increase readability.

Figure 7: the caption lacks information on panel e, f and g.

A: We have added a description for the respective panels in the caption.

Minor comments

L21: Could be useful to give an indication of the typical timeline referred to here.

A: The timeline is described in **L26-31**. We change the phrasing to make the link between the sentences clearer.

L26: **"**According to their ~~conceptual model~~ **proposed timeline**, ...**"**

L69: The sentence is long and unclear, please rephrase. "The suite of Lagrangian observations available …"

A: We have made major revisions in the last paragraph of the Introduction to better highlight the novelty of the study, inspired by the reviewer's suggestions.

L72 -79 : "In this study, we extend the trajectory methodology in Svensson et al. (2023) on the WAI captured by HALO-(AC)3 on March 12, 2022 and find a similar column-like flow pattern. ~~The suite of Lagrangian observations available for this case makes it a suitable testbed for the development of a Lagrangian single-column modeling framework to study real WAI cases, as per Pithan et al. (2016, 2018)'s suggestions, using the Atmosphere-Ocean Single-Column Model (AOSCM, Hartung et al., 2018). We use the model to investigate the processes that drive the airmass transformation. We~~

~~compare our simulations to observations, ERA5 and IFS forecast data in order to assess the performance of the model and its potential as a tool to test and construct future model parameterizaton schemes.~~ **We develop a Lagrangian single-column modeling framework suitable for the study of real WAI cases, as per Pithan et al. (2016, 2018)'s suggestions. We use the Atmosphere-Ocean Single-Column Model (AOSCM, Hartung et al., 2018) and take into account the time-varying dynamic and surface conditions that are relevant for the Arctic airmass transformation. In this simple, novel framework we can investigate the physical drivers and timescales of the transformation, in isolation from the complex dynamics that are typically associated with warm-air intrusions. Through comparison with the large number of Lagrangian HALO-(AC)3 observations available for this case, as well as ERA5 and IFS forecast data we assess the model's performance and its potential as a tool for testing and developing future model parameterization schemes."**

L76: This section seems to be more of a weather description based on the observational data. Consider using a more descriptive section title.

A: We have renamed Sect. 2.1 to **"Case Study and** observations**"** . This section offers details about the time and location of the studied warm-air intrusion episode as well as information about the observations used for the analysis. A proper weather description is not given until later in Sect. 3.1.

L147: Clarify the connection between the two sentences

A: L171-173 : "~~The presence of snow on ice, not allowed in OpenIFS, has also been~~ **Additionally, the use of the sea ice model LIM3 allows the presence of snow on ice, which has been** shown to mitigate surface energy and near-surface air-temperature biases (Pithan et al., 2016)**"**

L155: Rephrase as "The modeled profiles at the final timestep of the previous simulation are used as initial conditions for the following simulation at each transition point between surface regimes."

A: Done (**L181-182**)

L156: Rephrase as "Two additional preparatory simulations are performed over each sea-ice leg. The first one using… "

A: Done (**L182-183**)

L165: Consider whether the information on climatological perspective could be better placed somewhere else.

A: This is the only part of the manuscript where the large-scale setting is discussed and therefore the climatological perspective of the flow configuration is only be relevant here.

L189: Rephrase "To the degree that this feature is common along WAI, …. " It is unclear whether this is a statement or a question on whether they are common.

A: We rephrase:

L216-217: "~~To the degree that this feature is common among WAIs,~~**, although further investigation is needed in order to determine how common it is among WAIs. Nevertheless, when this feature is encountered,** it facilitates the exploration of Arctic airmass transformations with simple 1D models such as the AOSCM."

L240. Section 3.3 contains mostly method material and should be moved to the methods section

A: We have moved the first two paragraphs of Sect. 3.3 to method sections 2.1 and 2.4. Changes can be found in:

L113-120 : "At the point of initialization, 96% of the total moisture content of the column is contained in the lowest 5 km. Therefore we consider the airmass transformation to be taking place within a 5 km deep layer above the surface and do not examine trajectories at lower pressure levels. Additionally, we do not seek for vertical alignment in trajectories at pressure levels higher than 900 hPa, that may fall within the boundary layer. This is due to the expectation that the friction- induced wind shear and veer (vertical gradients in wind speed and direction respectively) near the surface would cause air-parcels to move in different directions to the rest of the airmass. However, we also expect the interaction with the changing surface properties through vertical mixing to be driving changes in the boundary layer properties more strongly than any potential differential advection, leading us to treat the boundary layer as part of the advected air-column."

and

L152- 163 : "~~In order to follow the Lagrangian evolution of the airmass with the AOSCM, we set the advective tendencies to zero, inhibiting the inflow(outflow) of heat, moisture or momentum from(to) the ambient atmosphere.~~ **For Lagrangian applications, the AOSCM requires information on the airmass path which, in our case, is indicated by the vertically aligned trajectory ensemble (Sect. 2.2).** The atmospheric column is made aware of its poleward advection through the temporally varying surface conditions and large-scale dynamical forcing, the details of which (surface type, surface temperature and large-scale subsidence) ~~along the predesignated~~ **are** obtained from ERA5 reanalysis data **along the predesignated airmass tracks** ~~(Sect. 2.2).~~ **The alongstream conditions may slightly vary between the individual trajectories, despite the spatial and temporal proximity within the ensemble. Therefore, we use all initial profiles paired with their respective alongstream surface and dynamic conditions to perform ensemble simulations. This approach gives some insight on both the mean characteristics of the airmass transformation, but also reveal its sensitivity to potential variability in initial conditions and forcing factors.**

We set the advective tendencies to zero, inhibiting the inflow(outflow) of heat, moisture or momentum from(to) the ambient atmosphere. Pressure-gradient forcing leads to the emergence of inertial oscillations close to the surface, which lead to unphysical surface fluxes of heat and momentum. In order to suppress these spurious oscillations we nudge the horizontal wind to the ERA5 profiles throughout the entire column and set the nudging timescale (τ_{nudge}) to be equal to the model timestep (15 min)**"**

L259: The reference to Fig. 4 is too early, the reader doesn't know what to look for yet.

A: We have removed the reference.

L266: Expand on this first description of Fig. 4, guide the reader through the details of the figure.

A: All figures are now introduced in detail in the introduction of Sect. 3.3 and the figure's updated caption.

L317: Rephrase as "At the end of the simulation, uncertainty in the heat content grows as well, due to slight variations in the forcing among the trajectory."

A: See next comment.

L318: Unclear sentence: "The same behavior is exhibited by the airmass in …"

A: We have rewritten this paragraph and moved it upward to **L329-333** where the ensemble uncertainty is already presented to make the text less repetitive and more coherent.

L328-332: "The upward tilt of the perpendicular lines indicates greater variability in heat compared to moisture content, in contrast to the beginning of the simulation, when the opposite was true. This feature is more pronounced in the AOSCM simulations but also apparent in ERA5 and IFS-OF. The similarities among the different products in the evolution of the airmass mean properties and variability suggest that the AOSCM, if appropriately forced, is, able to represent the physical processes that drive the airmass transformation"

L325: It is currently unclear now whether the warm and moist airmass is confined within the boundary layer or if the boundary layer depth is additional information. Rephrase sentence.

A: We rephrase to clarify.

L346-347: "Our initial airmass appears to be warm and moist, primarily within the boundary layer which reaches a depth of just over 1 km on average (Fig. 5a), but also above it, extending up to around 3 km"

L362: Add a reference here

A: We added a reference to the AOSCM cross-sections.

L383-384: "ERA5 and the IFS-OF (Fig. 5 middle and right columns) show a similar airmass transformation time-line with that simulated by AOSCM **(Fig. 5 left column)."**

L391: Unclear what this statement means: "The ensemble mean AOSCM, ERA5 and IFS-OF profiles in the center of each dropsonde cluster."

A: We apologize for the incomplete sentence. We added:

L413-414: "The ensemble mean AOSCM, ERA5 and IFS-OF profiles **are taken** in the center of each dropsonde cluster**."**

We thank the reviewer once again for their thorough examination of the manuscript. We have also addressed all technical comments listed below in the revised version of the manuscript.

Technical comments

L43: Remove the double "and"

L50: sampling → sampled

L53: Connect to a narrative instead of “them” —> “… reveal the time-scales and processes that drive **them”**

L95: Connect to a narrative instead of “Their”

L143: Remove the last 6 words of the sentence: “for this part of the simulation”

L163: develops → developed

L190: Replace “while” with “then/and”

L214: Move the reference to Fig. 3d to the back of the sentence.

L216: Missing space

L250: Add: “stems from two reasons”, or drop the point markings.

L259: Connect to narrative instead of “Their”

L327: Drop the additional “the” before “threshold”

L387: Drop the additional “observed”

L416: therefore → replace with “thus”

L421: moistest → “most moist/humid”

L429: insert at → to zero at the top

L458: misplaced dot

L469: mid-April → mid-March

***Note:** Please note that we have recalculated the temperature averages shown in Fig. 4 in the manuscript). In the previous version, the vertical averaging unintentionally gave greater weight to lower atmospheric levels due to the irregular vertical grid, resulting in higher values. The revised $\overline{T_{5km}}$ now properly accounts for vertical resolution.

While the updated temperature values appear generally lower, the structure of the curves remains largely unchanged. Therefore, the main characteristics of the airmass transformation remain clearly visible: slope flattening over the MIZ, similarities in the heat-to-moisture trends across datasets, variations in uncertainty, and close agreement in the final airmass state. Related numerical values and minor visual differences resulting from the new calculation are properly reflected in the revised text (Sect. 3.3.1 and 3.3.3). These adjustments are minor and do not affect our main conclusions.

Changes in the text include:

L287-288: “~~2.2~~ **-7.6** °C). IFS-OF shows a slightly **colder and** moister airmass ~~(by 0.4~~ **at around −7.7 °C and 13.8 kg m^{-2}**~~)~~ **respectively.”**

L290-292: “The overall changes sum up to ~~2.5~~ **approximately −2** °C for temperature and a mere **−**0.5 kg m^{-2} for moisture, on average, for the AOSCM and ERA5. For IFS-OF the respective changes are ~~2.3~~ **−2** ° C and −1 kg m^{-2} **.”**

L307-309: "The AOSCM shows a ~~1~~ **0.5** kg m−2 drop in IWV_{5km} ~~decrease in IWV5km and a 0.6 ∘C cooling,~~ while the **but no significant cooling. T**he standard deviation remains mostly unchanged.~~In ERA5, the T 5km∼IWV5km slope momentarily reverses, suggesting a short-lived heating of the 5 km layer upon the airmass entrance in the MIZ. By the end of the MIZ leg,~~ **The** ERA5 ~~heat and moisture drops to values comparable to the ones predicted by the AOSCM~~ **curve exhibits a similar flattening, showing a moisture loss similar to the one predicted by AOSCM (0.5 kg m^{-2}) but a slightly more pronounced cooling (∼ 0.2 ◦C). "**

References

1. ECMWF: IFS Documentation – Cy43r3, ECMWF, https://doi.org/10.21957/efyk72kl, dOI: 10.21957/efyk72kl, 2017.
2. Ehrlich, A., Crewell, S., Herber, A., Klingebiel, M., Lüpkes, C., Mech, M., Becker, S., Borrmann, S., Bozem, H., Buschmann, M., Clemen, H.-C., De La Torre Castro, E., Dorff, H., Dupuy, R., Eppers, O., Ewald, F., George, G., Giez, A., Grawe, S., Gourbeyre, C., Hartmann, J., Jäkel, E., Joppe, P., Jourdan, O., Jurányi, Z., Kirbus, B., Lucke, J., Luebke, A. E., Maahn, M., Maherndl, N., Mallaun, C., Mayer, J., Mertes, S., Mioche, G., Moser, M., Müller, H., Pörtge, V., Risse, N., Roberts, G., Rosenburg, S., Röttenbacher, J., Schäfer, M., Schaefer, J., Schäfler, A., Schirmacher, I., Schneider, J., Schnitt, S., Stratmann, F., Tatzelt, C., Voigt, C., Walbröl, A., Weber, A., Wetzel, B., Wirth, M., and Wendisch, M.: A comprehensive in situ and remote sensing data set collected during the HALO–(AC)3 aircraft campaign, Earth System Science Data, 17, 1295–1328, https://doi.org/10.5194/essd-17-1295-2025, publisher: Copernicus GmbH, 2025.
3. Hartung, K., Svensson, G., Struthers, H., Deppenmeier, A.-L., and Hazeleger, W.: An EC-Earth coupled atmosphere–ocean single-column model (AOSCM.v1_EC-Earth3) for studying coupled marine and polar processes, Geoscientific Model Development, 11, 4117–4137, https://doi.org/10.5194/gmd-11-4117-2018, publisher: Copernicus GmbH, 2018.
4. Paulus, F. M., Karalis, M., George, G., Svensson, G., Wendisch, M., and Neggers, R. A. J.: Airborne measurements of mesoscale divergence at high latitudes during HALO-(AC)3, https://doi.org/10.1175/JAS-D-24-0034.1, section: Journal of the Atmospheric Sciences, 2024.
5. Pithan, F., Ackerman, A., Angevine, W. M., Hartung, K., Ickes, L., Kelley, M., Medeiros, B., Sandu, I., Steeneveld, G.-J., Sterk, H. a. M., Svensson, G., Vaillancourt, P. A., and Zadra, A.: Select strengths and biases of models in representing the Arctic winter boundary layer over sea ice: the Larcform 1 single column model intercomparison, Journal of Advances in Modeling Earth Systems, 8, 1345–1357, https://doi.org/10.1002/2016MS000630, _eprint: https://onlinelibrary.wiley.com/doi/pdf/10.1002/2016MS000630, 2016.
6. Pithan, F., Svensson, G., Caballero, R., Chechin, D., Cronin, T. W., Ekman, A. M. L., Neggers, R., Shupe, M. D., Solomon, A., Tjernström, M., and Wendisch, M.: Role of air-mass transformations in exchange between the Arctic and mid-latitudes, Nature Geoscience, 11, 805–812, https://doi.org/10.1038/s41561-018-0234-1, number: 11 Publisher: Nature Publishing Group, 2018.

7. Rinke, A., Cassano, J. J., Cassano, E. N., Jaiser, R., and Handorf, D.: Meteorological conditions during the MOSAiC expedition: Normal or anomalous?, Elementa: Science of the Anthropocene, 9, 00 023, https://doi.org/10.1525/elementa.2021.00023, 2021.685

8. Rousset, C., Vancoppenolle, M., Madec, G., Fichefet, T., Flavoni, S., Barthélemy, A., Benshila, R., Chanut, J., Levy, C., Masson, S., and Vivier, F.: The Louvain-La-Neuve sea ice model LIM3.6: global and regional capabilities, Geoscientific Model Development, 8, 2991–3005, https://doi.org/10.5194/gmd-8-2991-2015, publisher: Copernicus GmbH, 2015.

9. Svensson, G., Murto, S., Shupe, M. D., Pithan, F., Magnusson, L., Day, J. J., Doyle, J. D., Renfrew, I. A., Spengler, T., and Vihma, T.: Warm air intrusions reaching the MOSAiC expedition in April 2020—The YOPP targeted observing period (TOP), Elem Sci Anth, 11, 00 016, https://doi.org/10.1525/elementa.2023.00016, 2023.

10. Vaisala: Vaisala Radiosonde RD41 datasheet in English, https://www.nirb.ca/portal/dms/script/dms_download.php?fileid=340414&applicationid=125718&sessionid=ka7asjkahsplnt1tq4rduoqbl1, accessed: 2025-03-24, 2020.

11. Viceto, C., Gorodetskaya, I. V., Rinke, A., Maturilli, M., Rocha, A., and Crewell, S.: Atmospheric rivers and associated precipitation patterns during the ACLOUD and PASCAL campaigns near Svalbard (May–June 2017): case studies using observations, reanalyses, and a regional climate model, Atmospheric Chemistry and Physics, 22, 441–463, https://doi.org/10.5194/acp-22-441-2022, publisher: Copernicus GmbH, 2022

12. Wendisch, M., Crewell, S., Ehrlich, A., Herber, A., Kirbus, B., Lüpkes, C., Mech, M., Abel, S. J., Akansu, E. F., Ament, F., Aubry, C., Becker, S., Borrmann, S., Bozem, H., Brückner, M., Clemen, H.-C., Dahlke, S., Dekoutsidis, G., Delanoë, J., De La Torre Castro, E., Dorff, H., Dupuy, R., Eppers, O., Ewald, F., George, G., Gorodetskaya, I. V., Grawe, S., Groß, S., Hartmann, J., Henning, S., Hirsch, L., Jäkel, E., Joppe, P., Jourdan, O., Jurányi, Z., Karalis, M., Kellermann, M., Klingebiel, M., Lonardi, M., Lucke, J., Luebke, A. E., Maahn, M., Maherndl, N., Maturilli, M., Mayer, B., Mayer, J., Mertes, S., Michaelis, J., Michalkov, M., Mioche, G., Moser, M., Müller, H., Neggers, R., Ori, D., Paul, D., Paulus, F. M., Pilz, C., Pithan, F., Pöhlker, M., Pörtge, V., Ringel, M., Risse, N., Roberts, G. C., Rosenburg, S., Röttenbacher, J., Rückert, J., Schäfer, M., Schaefer, J., Schemann, V., Schirmacher, I., Schmidt, J., Schmidt, S., Schneider, J., Schnitt, S., Schwarz, A., Siebert, H., Sodemann, H., Sperzel, T., Spreen, G., Stevens, B., Stratmann, F., Svensson, G., Tatzelt, C., Tuch, T., Vihma, T., Voigt, C., Volkmer, L., Walbröl, A., Weber, A., Wehner, B., Wetzel, B., Wirth, M., and Zinner, T.: Overview: quasi-Lagrangian observations of Arctic air mass transformations – introduction and initial results of the HALO-(AC)3 aircraft campaign, Atmospheric Chemistry and Physics, 24, 8865–8892, https://doi.org/10.5194/acp-24-8865-2024, publisher: Copernicus GmbH, 2024

13. Woods, C. and Caballero, R.: The Role of Moist Intrusions in Winter Arctic Warming and Sea Ice Decline, Journal of Climate, 29, 4473–4485, https://doi.org/10.1175/JCLI-D-15-0773.1, publisher: American Meteorological Society Section: Journal of Climate, 2016.

14. Zhang, Z., Ralph, F. M., Zou, X., Kawzenuk, B., Zheng, M., Gorodetskaya, I. V., Rowe, P. M., and Bromwich, D. H.: Extending the Center for Western Weather and Water Extremes

(CW3E) atmospheric river scale to the polar regions, The Cryosphere, 18, 5239–5258, https://doi.org/10.5194/tc-18-5239-2024, publisher: Copernicus GmbH, 2024.